TÜRKİYE CUMHURİYETİ
ADANA ALPARSLAN TÜRKEŞ SCIENCE AND TECHNOLOGY UNIVERSITY

GRADUATE SCHOOL
BIOENGINEERING DEPARTMENT

DESIGNING OF L-PROLINE SPECIFIC NANOPARTICLES FOR L-PROLINE DETECTION FROM HUMAN SERUM

MUSTAFA NERGİZ

M.Sc.

ADANA 2024

TÜRKİYE CUMHURİYETİ
ADANA ALPARSLAN TÜRKEŞ SCIENCE AND TECHNOLOGY UNIVERSITY

GRADUATE SCHOOL
BIOENGINEERING DEPARTMENT

DESIGNING OF L-PROLINE SPECIFIC NANOPARTICLES FOR L-PROLINE DETECTION FROM HUMAN SERUM

MUSTAFA NERGİZ

M.Sc.

THESIS ADVISOR
PROFESSOR GÖZDE BAYDEMİR PEŞİNT

ADANA, 2024

DECLARATION OF CONFORMITY

In this thesis study, which was prepared following the thesis writing rules of Adana Alparslan Türkeş Science and Technology University Institute of Graduate School, I declare that I provide all the information, documents, evaluations and results in accordance with scientific ethics and moral codes without resorting to any means or assistance that would be contrary to scientific ethics and traditions. I also declare that I refer to all of the articles I used in this study with appropriate references and accept all moral and legal consequences if a situation is found contrary to my statement regarding my work.

25/12/2023

[Signature]

Mustafa NERGİZ

ABSTRACT

DESIGNING OF L-PROLINE SPECIFIC NANOPARTICLES FOR L-PROLINE DETECTION FROM HUMAN SERUM

Mustafa NERGİZ

M.Sc., Department of Bioengineering

Supervisor: Prof. Dr. Gözde BAYDEMİR PEŞİNT

January 2024, 71 pages

Processes such as the detection and quantification of amino acids hold significant importance in biochemical analyses, particularly in the diagnosis of metabolic disorders. Among these amino acids, L-Proline has been identified as having significant relevance to various metabolic disorders in living organisms, particularly in human. Hyperprolinemia is a metabolic disorder that arises when the L-proline molecule is not effectively broken down due to deficiencies in proline oxidase or pyrroline-5 carboxylate dehydrogenase enzymes, resulting in an accumulation of L-Proline within the body. In individuals with Hyperprolinemia, there is a noticeable increase in L-Proline levels in both blood and urine, underlining the importance of accurately measuring and monitoring these levels in body fluids. To address the challenge of recognizing target molecules, such as proteins, peptides, amino acids, or ions, in complex environments with high selectivity, molecular imprinting emerges as a dependable technique that accomplishes this in a single step. In this study, molecularly imprinted nanoparticles that can selectively recognize the L-Proline molecule were synthesized. Hydroxyethyl methacrylate (HEMA) based nanoparticles were synthesized via emulsion polymerization technique and were characterized by scanning electron microscopy, zeta-sizer particle size analysis, surface area calculations, and Fourier Transform Infrared Spectroscopy (FTIR). Based on zeta-sizer analysis, the estimated diameters of Pro-MIP and NIP nanoparticles were determined to be approximately 27.51 nm and 20.66 nm, respectively. The adsorption of L-Proline onto nanoparticles from aqueous solutions was investigated in a batch system, and the maximum L-Proline adsorption capacity was determined to be 26.58 mg/g for Pro-MIP and 4.65 mg/g for NIP. The selectivity of L-Proline imprinted nanoparticles was successfully confirmed via Liquid Chromatography-Tandem Mass Spectrometry (LC-MS/MS), in the presence of

competing molecules (L-Histidine and L- Phenylalanine). Finally, Pro-MIPs were subjected to repeated adsorption-desorption cycles and it was demonstrated that Pro-MIPs can be used up to 10 times without significant decrease in selective adsorption capacity.

Keywords: L-Proline, hyperprolinemia, molecularly imprinted polymers, nanoparticles.

ÖZET

L-PROLİN MOLEKÜLÜNE ÖZGÜ NANOPARÇACIKLARIN İNSAN SERUMUNDAN L-PROLİN TESPİTİ İÇİN TASARLANMASI

Mustafa NERGİZ
Yüksek Lisans, Biyomühendislik Anabilim Dalı
Danışman: Prof. Dr. Gözde BAYDEMİR PEŞİNT
Ocak 2024, 71 sayfa

Amino asitlerin tespiti ve miktarının belirlenmesi gibi süreçler, özellikle metabolik bozuklukların teşhisinde biyokimyasal analizlerde önemli bir rol oynamaktadır. Bu amino asitler arasında, L-Prolin'in, özellikle insanlarda çeşitli metabolik bozukluklarla önemli bir ilişkiye sahip olduğu belirlenmiştir. Hiperprolinemi, L-prolin molekülünün prolin oksidaz veya pirolin-5 karboksilat dehidrogenaz enzimlerindeki eksiklikler nedeniyle etkili bir şekilde parçalanamadığı durumlarda ortaya çıkan bir metabolik bozukluktur, böylece vücut içinde L-Prolin birikmesine neden olur. Hiperprolinemiye sahip bireylerde, kan ve idrarda L-Prolin seviyelerinde belirgin bir artış gözlemlenir, bu da vücut sıvılarında bu seviyelerin doğru bir şekilde ölçülmesinin ve izlenmesinin önemini vurgular. Proteinler, peptitler, amino asitler, iyonlar, vb. hedef moleküllerin yüksek seçicilikle karmaşık ortamlarda tanınma zorluğuna çözüm olarak, moleküler kalıplama, bu işi tek bir adımda başaran güvenilir bir teknik olarak öne çıkar. Bu tez çalışmasında, L-Prolin molekülünü seçici bir şekilde tanıyabilen moleküler baskılanmış nanopartiküller sentezlenmiştir. Hidroksietil metakrilat (HEMA) tabanlı nanopartiküller, emülsiyon polimerizasyon tekniği kullanılarak sentezlenmiştir ve taramalı elektron mikroskobu, zeta-sizer parçacık boyutu analizi, yüzey alanı hesaplamaları ve Fourier Dönüşümü Kızılötesi Spektroskopisi (FTIR) ile karakterize edilmiştir. Zeta-sizer analizi sonuçlarına göre, Pro-MIP ve NIP nanopartiküllerin çapları sırasıyla yaklaşık 27.51 nm ve 20.66 nm olarak belirlendi. L-Prolin'in sulu çözeltilerden nanopartiküllere adsorpsiyonu batch sistemde incelendi ve maksimum L-Prolin adsorpsiyon kapasitesi Pro-MIP için 26.58 mg/g, NIP için ise 4.65 mg/g olarak belirlendi. L-Prolin baskılanmış nanopartiküllerin seçiciliği, yarışmacı moleküller (L-Histidin ve L-Fenilalanin) varlığında Sıvı Kromatografi-İkinci Kütle Spektrometrisi (LC-MS/MS) kullanılarak başarıyla doğrulandı. Son olarak, Pro-MIP'ler

tekrarlanan adsorpsiyon-desorpsiyon döngülerine tabi tutuldu ve Pro-MIP'lerin seçici adsorpsiyon kapasitesinde önemli bir azalma olmadan 10 kez kullanılabileceği gösterildi.

Anahtar Kelimeler: L-Prolin, hiperprolinemi, moleküler baskılanmış polimerler, nanopartiküller.

Dedication

To my beloved family…

ACKNOWLEDGEMENTS

I would like to express my heartfelt gratitude to my esteemed supervisor, Prof. Dr. Gözde BAYDEMİR PEŞİNT, for her invaluable guidance, unwavering support, and positive encouragement throughout the swift progress of this endeavor. Being her student fills me with great pride.

I extend my sincere thanks to Okan ZENGER, for generously sharing his knowledge and expertise at every stage of this study. His guidance and support, especially during challenging moments, have been instrumental.

I would like to express my gratitude to Burcu EREN YÜNGEVİŞ and Pırıl ARISOY for their support and friendship throughout my thesis studies.

Lastly, I am profoundly grateful to my beloved family for their enduring support, continuous encouragement, and limitless motivation that have played a crucial role not only in this project but throughout my life.

I am grateful for the support provided by ATU BAP Coordination Unit with project number 21303015 in the completion of this thesis.

TABLE OF CONTENTS

LIST OF FIGURES

LIST OF TABLES

LIST OF ABBREVIATIONS

MIP	**:** Molecularly Imprinted Polymer
MIT	**:** Molecular Imprinting Technology
NaCl	**:** Sodium Chloride
Ultrapure water	**:** UW
HPLC	**:** High-performance liquid chromatography
MS	**:** Mass Spectrometry
FTIR	**:** Fourier transform infrared spectroscopy
SEM	**:** Scanning electron microscope
PBS	**:** Phosphate - buffered saline
EGDMA	**:** Ethylene Glycol Dimethacrylate
PVA	**:** Poly(Vinyl Alcohol)
APS	**:** Ammonium persulfate
SDS	**:** Sodium Dodecyl Sulfate
VIM	**:** 1-Vinylimidazole
HEMA	**:** 2-Hydroxyethylmethacrylate
p(HEMA)	**:** Poly(2-Hydroxyethylmethacrylate)
NP	**:** Nanoparticle
NIP	**:** Non-imprinted Nanoparticle
UV	**:** Ultraviolet

LIST OF SYMBOLS

µL : Microliter
µm : Micrometer
nm : Nanometer
mL : Milliliter
mg : Milligram
ng : Nanogram
pg : Picogram
cm : Centimeter
L : Liter
t : Temperature
sec : Second
Min : Minute
h : Hour
eq. : Equation
M : Molarity
°C : Celsius degree
CO_2 : Carbon Dioxide
k : Selectivity coefficient
IF : Imprinting Factor

1. INTRODUCTION

Processes such as the detection and quantification of amino acids play a significant role in biochemical analyses, especially in the diagnosis of metabolic disorders (Gałęzowska et al., 2021; Sandlers, 2019; R. Y. Wang et al., 2013). Proline (symbol Pro or P) is one of the 20 amino acids that constitute proteins. Proline is classified as a proteinogenic amino acid, meaning it is an organic acid used in the biosynthesis of proteins, even though it lacks a primary amino group in its structure. Unlike all other amino acids, which carry a primary amino group, proline is classified as an aliphatic amino acid because it forms a ring with three carbon atoms in its side chain, connecting to the nitrogen atom in the peptide bond (Allen et al., 2004; Szabados & Savouré, 2010a). Proline is not essential in humans, as the body can synthesize it from the non-essential amino acid L-glutamate. Proline is encoded by all codons starting with CC (CCU, CCC, CCA, and CCG) (Allen et al., 2004; Alvarez et al., 2022; Szabados & Savouré, 2010a). The molecule L-proline has been reported to be associated with various metabolic disorders in living organisms. In plants, the accumulation of proline is a common physiological response to various stresses but is also part of the development program in reproductive tissues, such as pollen (Mitsubuchi et al., 2008; Van Hove & Thomas, 2013; Yao & Han, 2022). Hiperprolinemia is a metabolic disorder that results from the improper breakdown of proline molecules by proline oxidase or pyrroline-5-carboxylate dehydrogenase enzymes, leading to the accumulation of proline in the body. Proline levels in blood and urine increase in this condition. Kidney damage is observed in type I hiperprolinemia, and both types result in intellectual disability. Therefore, the detection of L-proline is crucial for diagnosis and treatment (Jacquet et al., 2005; Mitsubuchi et al., 2008, 2014; Namavar et al., 2021).

Molecular imprinting is a reliable technique used to selectively recognize a target molecule (e.g., protein, peptide, amino acid, ion, etc.) from a complex environment in a single step with high selectivity (Singabraya et al., 2012; Ye et al., 1999; Zenger & Peşint, 2022). Molecularly imprinted polymers are primarily designed in three steps: an interaction occurs between functional monomers and the template molecule; the surroundings of the functional monomer-template molecule complex are polymerized in the presence of cross-linkers and monomers; finally, the template molecule is removed from the polymeric structure, leaving specific cavities

in the polymer with shape and chemical structure memory for the desired molecule (Andaç et al., 2016; Ye et al., 1999; Yıldırım & Baydemir Peşint, 2021; Zenger & Peşint, 2022). Molecularly imprinted polymers are reusable materials that can be stored for several years without any change in their performance. Due to their advantages, they are used as synthetic recognition elements in various applications such as diagnostics, separation, purification, healthcare, food, environment, etc (Alexander et al., 2006; Andaç et al., 2016; L. Chen et al., 2011).

In this thesis study, L-proline-imprinted nanoparticles (Pro-MIPs) were synthesized for the determination of L-proline from aqueous solutions, body fluids, and plant extracts. HEMA-based nanoparticles were prepared using different ratios of cross-linkers, functional monomers, and the target molecule. The synthesized polymeric materials were Characterized by scanning electron microscopy (SEM), zeta-sizer particle size analysis, surface area calculations, and Fourier Transform Infrared Spectroscopy (FTIR). After the synthesis of nanoparticles, the template molecule (L-proline) were desorbed from the binding sites using appropriate buffers, thus creating regions in the polymer that can specifically recognize the L-proline molecule. Subsequently, the adsorption of L-proline from aqueous solutions were investigated in relation to recognition sites. Additionally, the selectivity of L-proline-imprinted nanoparticles were studied in the presence of competing molecules. In addition, the adsorption of L-proline from body fluids were investigated directly. As a control group, nanoparticles without the template molecule (NIP) were synthesized and used in adsorption studies, and the results were compared. Finally, the synthesized Pro-MIPs were subjected to repeated adsorption-desorption cycles to test their reusability.

In this thesis study, nanoparticles specifically recognizing the L-proline molecule, which serves as an indicator for various metabolic disorders, were synthesized using emulsion polymerization technique. There is no study in the literature using molecular imprinting techniques for the direct determination of L-proline from body fluids, and this study can pave the way for the preparation of polymeric materials capable of achieving this goal and can contribute significantly to the literature with further research. This study will be pioneering and open the doors to new methods in the field.

2. LITERATURE REVIEW

2.1. Amino Acids: The Building Blocks of Life

Amino acids are the building blocks of life, serving as the essential constituents of proteins and playing a wide range of critical roles in living organisms. When we refer to amino acids as the "building blocks of life," we are acknowledging their central role in constructing and maintaining the remarkable complexity of living organisms (Johnson & Korley, 2012; Kitadai & Maruyama, 2018).

Amino acids are characterized by a central carbon atom, often called the α-carbon, bonded to four distinct groups: a hydrogen atom, an amino group ($-NH_2$), a carboxyl group (-COOH), and a side chain known as the R-group. It's the R-group that distinguishes one amino acid from another, granting each its unique identity and functionality. With over 20 naturally occurring amino acids, this diversity of R-groups allows for the vast array of proteins in living organisms, each designed to perform specific tasks (Bojarska et al., 2019; Maity et al., 2023).

Proteins, composed of long chains of amino acids, serve as the workhorses of cells. They function as enzymes catalyzing biochemical reactions, structural components maintaining cellular integrity, receptors for cellular communication, and much more (Clark & Radivojac, 2011; G. Wu, 2009). The specific order of amino acids in a protein, which is controlled by our genes, decides how it looks and what it does. Even a tiny change in this order can cause big problems, like diseases or changes in how our body works. The role of amino acids goes beyond protein synthesis (Clark & Radivojac, 2011; Ng & Henikoff, 2006; G. Wu, 2009). They are also involved in neurotransmission, serving as the precursors for important neurotransmitters like serotonin and dopamine. Amino acids play a role in energy metabolism, serving as intermediaries in pathways such as the citric acid cycle. Furthermore, they contribute to the body's immune response, regulate gene expression, and even serve as signaling molecules in cell-to-cell communication (Bröer, 2022; P. Li et al., 2007; Neumann-Staubitz & Neumann, 2016; Ng & Henikoff, 2003).

Amino acids are the fundamental components of life. Their various shapes and abilities to do different jobs are incredibly important in biology. Whether in tiny bacteria or in complex humans, amino acids are like the essential builders that create life (Bojarska et al., 2019; Johnson & Korley, 2012; Kitadai & Maruyama, 2018; G. Wu, 2009).

2.1.1. Classification of amino acids

Amino acids can be classified into several categories based on their chemical properties and physiological roles. The primary classifications include:

2.1.1.1. Essential vs. non-essential amino acids

Essential amino acids cannot be synthesized by the human body and must be obtained through the diet. There are nine essential amino acids: histidine, isoleucine, leucine, lysine, methionine, phenylalanine, threonine, tryptophan, and valine. Non-essential amino acids are those that the body can synthesize on its own, and dietary intake is not strictly necessary. Examples include alanine, aspartic acid, proline, and glutamine (Deschepper & DeGroote, 1995; Heger, 2003; Kosiol et al., 2004; Mertz et al., 1952; Takahashi et al., 2011).

2.1.1.2. Polar vs. non-polar amino acids

Amino acids are categorized based on the polarity of their side chains (R-groups). Polar amino acids have hydrophilic R-groups, while non-polar amino acids have hydrophobic R-groups. This classification is crucial for understanding their interactions within biological systems (Kosiol et al., 2004; Taylor, 1986; Volkenstein, 1965).

2.1.1.3. Acidic vs. basic amino acids

Amino acids can also be categorized as acidic or basic, based on the charge of their R-groups at physiological pH. Acidic amino acids include aspartic acid and glutamic acid, which have negatively charged R-groups. Basic amino acids include lysine, arginine, and histidine, which have positively charged R-groups (Mjalli, 2016; Taylor, 1986).

2.1.2. Structure and function of amino acids

Amino acids are small organic molecules composed of carbon (C), hydrogen (H), oxygen (O), and nitrogen (N) atoms. Each amino acid consists of a central carbon atom, called the alpha carbon (α-carbon), bonded to four different chemical groups: an amino group ($-NH_2$), a carboxyl group (-COOH), a hydrogen atom (-H), and a unique side chain or R group. It's the R group that distinguishes one amino acid from another (Bojarska et al., 2019; Maity et al., 2023).

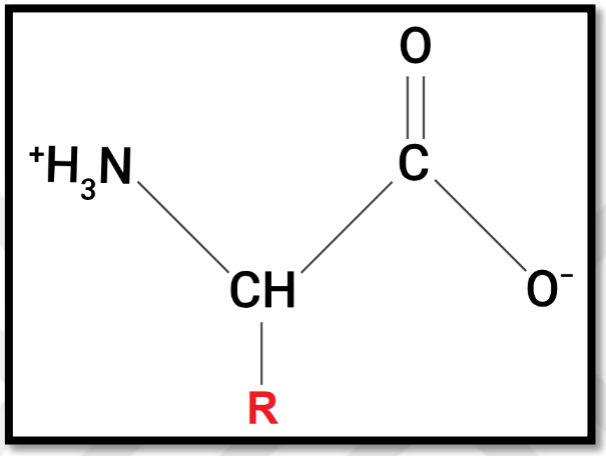

Figure 2.1. General molecular structure of amino acids.

There are 20 different amino acids that are commonly found in proteins, and they vary in the structure of their R groups. These variations give each amino acid its distinct properties and determine how it interacts with other molecules (Bojarska et al., 2019; Taylor, 1986).

Vital roles of amino acids in living organisms are given below:

1. Protein synthesis: Amino acids are the building blocks of proteins. During protein synthesis, amino acids are linked together through peptide bonds to form polypeptide chains. The sequence of amino acids in a polypeptide determines the protein's structure and function (Bojarska et al., 2019).

2. Enzymes and catalysts: Many enzymes are proteins composed of specific amino acid sequences. These enzymes catalyze biochemical reactions, facilitating processes like digestion,

cellular respiration, and DNA replication (P. Li et al., 2007; R. Y. Wang et al., 2013; G. Wu, 2009).

3. Structural components: Collagen, a fibrous protein, is rich in the amino acid glycine and provides structural support to connective tissues like skin, bones, and tendons. Keratin, another protein, is composed of cysteine-rich amino acids and is a major component of hair and nails (G. Wu, 2009).

4. Neurotransmitters: Amino acids such as glutamate and gamma-aminobutyric acid (GABA) serve as neurotransmitters in the nervous system, transmitting signals between nerve cells and regulating brain function (Yao & Han, 2022).

5. Immune response: Amino acids like arginine and glutamine play pivotal roles in immune function. Arginine is essential for the production of nitric oxide, a molecule involved in immune defense, while glutamine fuels the rapid proliferation of immune cells during infection (P. Li et al., 2007).

6. Energy metabolism: Amino acids can be broken down to produce energy when carbohydrates and fats are scarce. However, this process is typically reserved for times of dietary deficiency or intense physical activity (G. Wu, 2009).

7. Hormones and signaling molecules: Amino acids are involved in the synthesis of hormones and signaling molecules. For instance, tyrosine is a precursor to thyroid hormones, while tryptophan is a precursor to serotonin, a neurotransmitter that regulates mood (G. Wu, 2009).

2.2. Introduction to Proline

Among amino acids, proline stands out as a truly unique amino acid. One of the defining features that sets proline apart from other amino acids is its distinctive structural arrangement. While most amino acids have a linear backbone, proline forms a cyclic structure, creating a closed ring. This cyclic nature results from the attachment of its side chain (the R-group) to the nitrogen atom in the amino group, creating a five-membered ring (X. Liang et al., 2013; Szabados & Savouré, 2010a).

The unique circular shape of proline brings about some interesting characteristics. Firstly, it restricts the flexibility of the chemical bond that links proline within a protein sequence, which in turn impacts the overall shape of the protein. This structural limitation can be beneficial in particular protein functions, like the folding and stability of the protein (Bennick, 1987; Kay et al., 2000; Szabados & Savouré, 2010b).

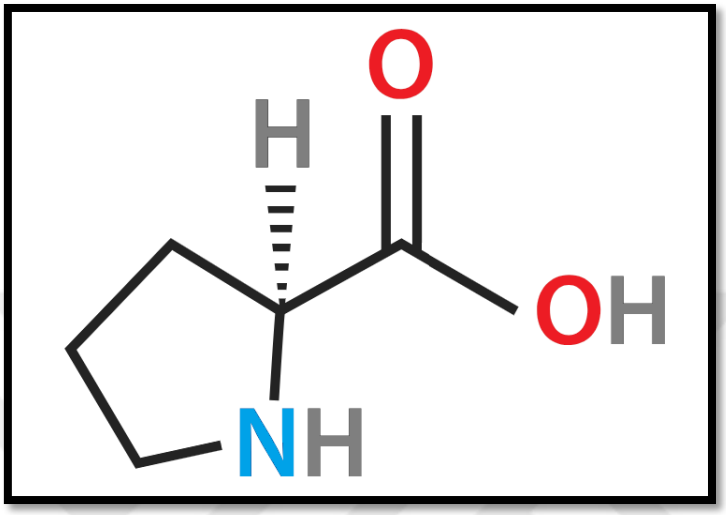

Figure 2.2. General molecular structure of proline amino acid.

2.2.1. The role of proline in protein structure

The unusual structure of proline also affects how proteins look in three dimensions when it's a part of them. When proline is in a protein, it can make the chain bend or kink. This is especially significant in proteins such as collagen, where proline's special shape helps create the protein's triple helix structure. This structure gives strength to tissues like skin, tendons, and cartilage (Bennick, 1982; Hayat et al., 2012). Moreover, proline often plays a role in protein domains and motifs involved in protein-protein interactions. It can act as a "hinge" residue, facilitating the bending or folding of proteins critical for their functions. Additionally, proline-rich regions in proteins are known to mediate interactions with other molecules, including DNA and RNA, highlighting proline's versatility in biological processes beyond protein structure (Bennick, 1982; Hayat et al., 2012; X. Liang et al., 2013).

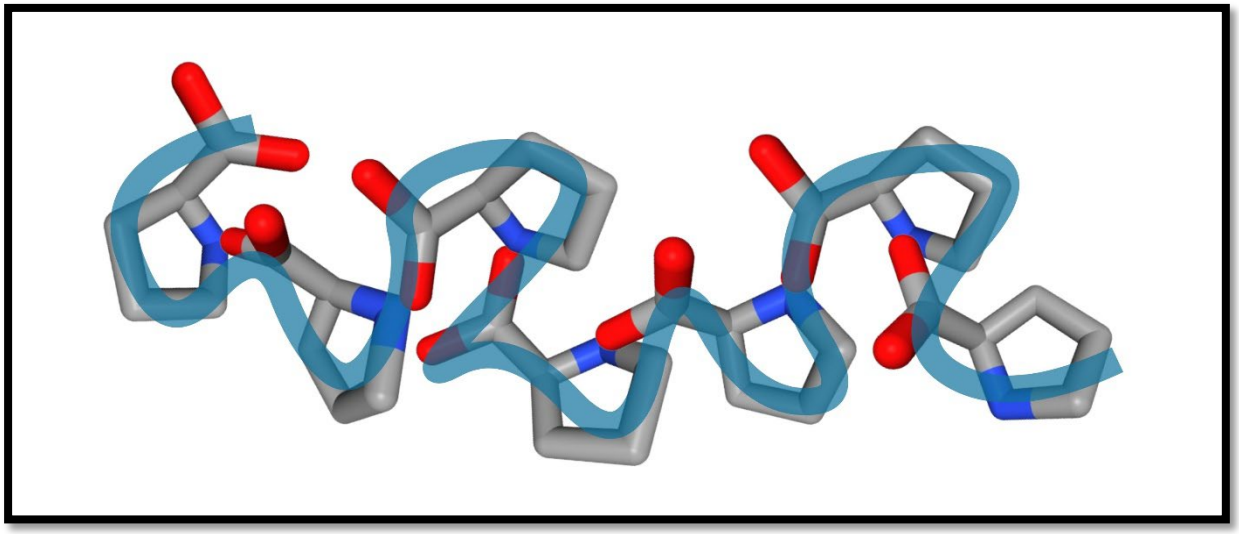

Figure 2.3. Representative illustration depicting the influence of proline amino acid on protein folding.

2.2.2. Function in Cellular Processes

Beyond its role in protein structure, proline is involved in various cellular processes. In particular, proline plays a crucial role in stress response mechanisms. During environmental stressors like drought, high salinity, or extreme temperatures, proline levels often increase in plant cells. This elevation of proline concentration acts as a protective mechanism, helping to stabilize cellular structures and maintain osmotic balance in challenging conditions (Bennick, 1982; Hayat et al., 2012; Kay et al., 2000).

Proline is also a key component in the biosynthesis of certain neurotransmitters and other biologically active molecules. In humans, proline serves as a precursor to the neurotransmitter glutamate and plays a role in the synthesis of collagen, an essential protein for connective tissues and wound healing (Hayat et al., 2012; X. Liang et al., 2013).

Among the many amino acids, proline is a truly special molecule. Its circular shape, the way it affects how proteins are shaped, and its roles in dealing with stress and cell functions make it an important part of biology. Whether it helps keep our connective tissues strong or helps us deal with stress, proline's special qualities show how complex and diverse the building blocks

of life are. Ongoing research is revealing more about proline's many roles in biology, showing how important it is for our health, understanding diseases, and the processes that keep us alive (Bennick, 1987; Hayat et al., 2012; Szabados & Savouré, 2010b).

2.2.3. L-proline and D-proline

L-proline and D-proline are two mirror-image isomers known as enantiomers. These enantiomers, often referred to as "chiral" forms, exhibit distinct structural and biochemical differences, underlining the significance of stereochemistry in biochemistry and biology (Casado et al., 2012; Kampel et al., 1990). Chirality refers to the property of molecules that have mirror-image isomers that cannot be superimposed onto each other. In the case of amino acids, this chirality primarily arises from the asymmetry of the central carbon atom, known as the alpha (α) carbon (Casado et al., 2012; D. Li et al., 2018; Q. Wang et al., 2015).

In the L-form of an amino acid, the amino group (-NH2) is positioned on the left side of the α carbon when viewed in a Fischer projection, while in the D-form, it is positioned on the right side. These mirror-image forms, while sharing the same chemical formula, exhibit differences in their three-dimensional structures, which can lead to vastly different interactions within biological systems (S. Chen et al., 2016; Y. Zhang et al., 2013).

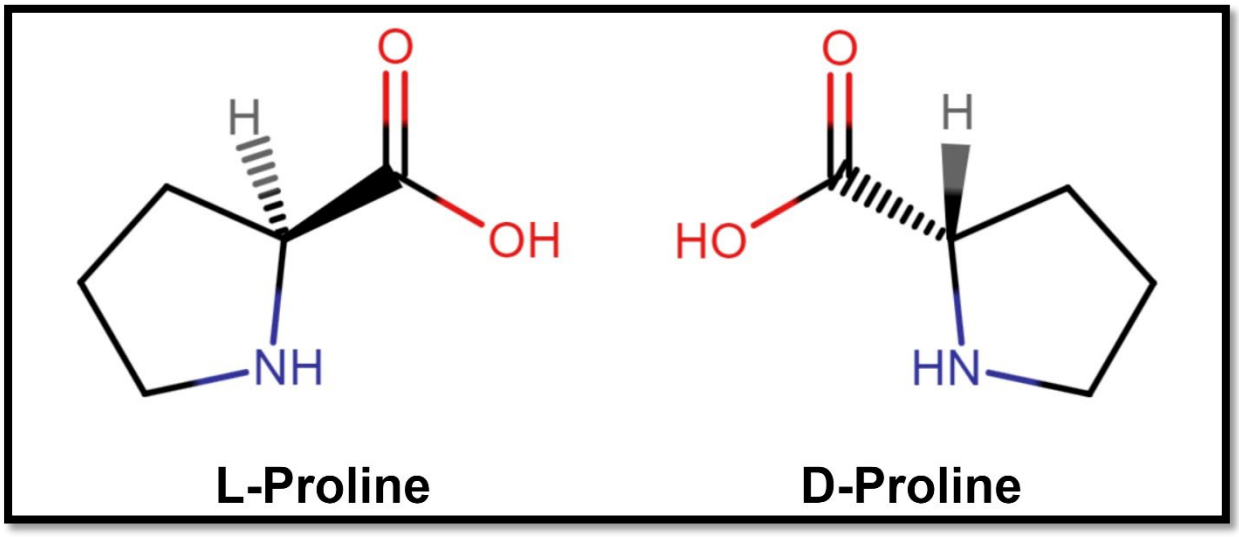

Figure 2.4. Molecular structures of L-Proline and D-Proline.

L-Proline is the naturally occurring and biologically active form of proline found in proteins and living organisms. Its distinct structure contributes to the unique properties of proteins that incorporate it into their sequences. For instance, L-proline is often found in turns or bends in protein structures, where its cyclic structure introduces kinks in the polypeptide chain. This conformational change can have significant effects on protein folding, stability, and function. On the other hand, D-proline is the enantiomer of L-proline, and while it is less commonly encountered in biological systems, it has its own distinct roles. D-Proline is sometimes found in the cell walls of certain bacteria and in the synthesis of specific antibiotics. Its structural differences can confer unique properties that are exploited in these biological contexts (Casado et al., 2012; Kampel et al., 1990; Y. Zhang et al., 2013).

The chiral nature of L-proline and D-proline highlights the exquisite selectivity of biological systems. Enzymes, for instance, are highly specific in recognizing and interacting with particular enantiomers. This specificity is often attributed to the shape and arrangement of functional groups around the chiral center (Casado et al., 2012; D. Li et al., 2018; Q. Wang et al., 2015).

The consequences of mistaking L-proline for D-proline (or vice versa) can be profound. In some cases, the presence of the incorrect enantiomer in a protein can render it nonfunctional or even detrimental to the organism. This selectivity at the molecular level underscores the critical importance of stereochemistry in biology (S. Chen et al., 2016; Kampel et al., 1990; Q. Wang et al., 2015).

2.2.3.1. The role of L-Proline in protein structure and function

Proteins are the workhorses of biology, carrying out plenty of functions in living organisms. From enzymes that catalyze chemical reactions to structural proteins that provide strength and stability to cells, the diverse roles of proteins are essential for life. At the heart of protein structure and function lies the remarkable amino acid L-proline, which plays a pivotal role in shaping and maintaining the intricate three-dimensional world of proteins (Adzhubei et al., 2013; Morgan & Rubenstein, 2013; Srinivas & Balasubramanian, 1995).

Protein folding is a highly organized process where a chain of amino acids takes on a specific 3D shape. L-proline, a unique type of amino acid, plays a vital role in this process (Adzhubei et al., 2013). It acts like a building block that can bend or twist the protein chain. These bends and twists created by L-proline help determine the protein's final shape. Sometimes, parts of proteins that have a lot of L-proline are crucial for their function. For instance, in collagen, the body's most common protein that's essential for tissues like skin, bones, and tendons, L-proline is needed to make collagen's unique triple helix structure, which gives strength to these tissues (Green & Lowther, 1959; Karna et al., 2020; P. Li & Wu, 2018).

L-proline is important for more than just the structure of proteins. It often helps proteins interact with each other, which is essential for many cell activities. Regions of proteins rich in L-proline can work like flexible hinges or spots that allow proteins to move and change shape (Adzhubei et al., 2013). These regions make it possible for proteins to connect with other molecules, like DNA, RNA, and other proteins. This way, L-proline helps regulate cell functions, like passing signals, controlling genes, and building larger protein groups (Adzhubei et al., 2013; Donohue & Trueblood, 1952; Mahoney et al., 1997).

In light of this, L-proline stands out as a vital element. Its distinctive structural features, like its circular arrangement and capacity to create bends in protein chains, make it an essential part of the biological machinery. Whether it's ensuring the strength of connective tissues or facilitating important protein interactions, L-proline plays a diverse and critical role in the world of proteins. Recognizing the central importance of L-proline not only deepens our understanding of protein biology but also highlights the fascinating complexities of life at the molecular level (Adzhubei et al., 2013; P. Li & Wu, 2018; Mahoney et al., 1997; Srinivas & Balasubramanian, 1995).

2.2.4. L-Proline in human health

L-Proline plays a crucial role in human health, contributing to various physiological processes that are essential for our well-being. Beyond its structural role in proteins, L-proline also serves

as a valuable biomarker, offering insights into specific health conditions and providing a window into our overall state of health (Hu et al., 2008; Vettore et al., 2021; G. Wu et al., 2011).

L-Proline is involved in several fundamental aspects of human physiology:

1. Collagen Formation: L-Proline is a key component of collagen, the most abundant protein in the human body. Collagen is responsible for providing structural support to various tissues, including skin, tendons, ligaments, and blood vessels. Without L-proline, the synthesis and maintenance of collagen would be compromised, potentially leading to connective tissue disorders and skin-related issues (Green & Lowther, 1959; Karna et al., 2020; Mitran et al., 2015).

2. Wound Healing: L-Proline plays a critical role in wound healing by assisting in the synthesis of collagen and other extracellular matrix components. It helps in tissue repair, ensuring that wounds close properly and scar formation is minimized (Albaugh et al., 2017; Ponrasu et al., 2013).

3. Immune System Support: L-Proline is involved in the proliferation of immune cells and the production of antibodies, contributing to a robust immune response against infections and diseases (P. Li et al., 2007; Patriarca et al., 2021; Zharkova et al., 2018).

4. Neurotransmitter Synthesis: L-Proline serves as a precursor for the synthesis of important neurotransmitters like glutamate and gamma-aminobutyric acid (GABA), which play key roles in brain function and mood regulation (Hill & Nemoto, 2016; Patriarca et al., 2021; Wyse & Netto, 2011).

Beyond its roles in various physiological processes, L-Proline also serves as a biomarker—a measurable indicator of specific health conditions or bodily functions. Here are some instances where L-Proline's levels can offer valuable insights into our health:

1. Collagen Disorders: Reduced levels of L-proline may be indicative of collagen disorders, such as Ehlers-Danlos syndrome or scurvy, where collagen synthesis is impaired. Monitoring

L-proline levels can aid in diagnosing and managing these conditions (Albaugh et al., 2017; Beighton, 1970; Karna et al., 2020; Steinmann et al., 2002).

2. Connective Tissue Health: L-Proline levels can reflect the health of connective tissues. Low L-proline levels may suggest connective tissue weaknesses or injuries, while elevated levels could be associated with increased collagen production during tissue repair (Albaugh et al., 2017; Ponrasu et al., 2013).

3. Neurological Disorders: Dysregulation of L-proline metabolism may be linked to certain neurological disorders. Monitoring L-proline levels can provide valuable information in the context of research and clinical investigations into conditions like schizophrenia and epilepsy (Hill & Nemoto, 2016; Wyse & Netto, 2011).

4. Nutritional Status: L-Proline levels can be influenced by dietary factors. Adequate dietary intake of proline-rich foods, such as meat, dairy, and certain plant sources, is important for maintaining healthy L-proline levels (Deschepper & DeGroote, 1995; P. Li & Wu, 2018).

5. L-Proline Accumulation: A deficiency in one of the enzymes involved in proline metabolism can lead to the accumulation of proline in the body. Hyperprolinemia is a rare metabolic disorder characterized by elevated levels of the amino acid proline in the blood and urine (Jacquet et al., 2005; Mitsubuchi et al., 2014; Namavar et al., 2021).

There are two main types of hyperprolinemia, each associated with a specific enzyme deficiency:

Type I Hyperprolinemia (HP-I): This form of hyperprolinemia is caused by a deficiency of the enzyme pyrroline-5-carboxylate dehydrogenase (P5CDH), which is involved in the conversion of pyrroline-5-carboxylate (P5C) to L-glutamate. As a result, P5C accumulates and is converted to proline, leading to elevated proline levels. Type I hyperprolinemia is typically considered a benign condition with few or no symptoms. It is often detected incidentally during routine blood tests (Jacquet et al., 2005; Mitsubuchi et al., 2014; Namavar et al., 2021).

Type II Hyperprolinemia (HP-II): In contrast to Type I, Type II hyperprolinemia is associated with a more severe deficiency, often involving both P5CDH and another enzyme called pyrroline-5-carboxylate reductase (P5CR). This form of hyperprolinemia can lead to neurological symptoms, intellectual disability, developmental delays, and behavioral issues. The severity of symptoms can vary among affected individuals (Jacquet et al., 2005; Mitsubuchi et al., 2014; Namavar et al., 2021).

The diagnosis of hyperprolinemia is typically made through blood and urine tests that reveal elevated levels of proline and P5C. Genetic testing can confirm the specific enzyme deficiency and help differentiate between Type I and Type II Hyperprolinemia (Jacquet et al., 2005; Mitsubuchi et al., 2014).

Treatment for hyperprolinemia often involves dietary management and addressing any associated symptoms. In Type I hyperprolinemia, dietary restrictions may not be necessary as the condition is generally benign. However, in Type II hyperprolinemia, a proline-restricted diet may be recommended to reduce the buildup of proline and P5C. In cases with neurological symptoms, additional interventions and therapies may be required to manage developmental delays and behavioral issues (Mitsubuchi et al., 2014; Namavar et al., 2021).

It's important to note that hyperprolinemia is a rare condition, and the severity of symptoms can vary widely among affected individuals. Early diagnosis and appropriate management are crucial for optimizing the long-term outcomes and quality of life for those with Type II hyperprolinemia. Genetic counseling may also be recommended for families with a history of the disorder to assess the risk of passing it on to future generations (Jacquet et al., 2005; Mitsubuchi et al., 2014; Namavar et al., 2021).

2.2.5. Quantitative analysis of L-Proline

The accurate detection and quantification of L-Proline are critical in various fields, including biochemistry, agriculture, and clinical diagnostics (Ábrahám et al., 2010; Forlani & Funck,

2020; Troll & Lindsley, 1955; Watkins et al., 2006). Several analytical techniques and methods are employed to accomplish this task. High-performance liquid chromatography (HPLC) is a commonly used method, where L-Proline can be separated and quantified based on its unique chemical properties. Additionally, mass spectrometry (MS) provides a powerful tool for both qualitative and quantitative analysis of L-Proline, offering high sensitivity and specificity. Spectrophotometric assays, such as the ninhydrin method, are widely employed for their simplicity and efficiency in detecting L-Proline based on colorimetric changes. Enzymatic assays utilizing specific enzymes that interact with L-Proline have also proven effective. Each of these techniques has its advantages and limitations, allowing researchers and analysts to choose the most suitable method depending on their specific needs and the sample matrix under investigation (Ábrahám et al., 2010; Chang et al., 2010; Forlani & Funck, 2020; M Hasanzadeh et al., 2018; Troll & Lindsley, 1955; Y. Wu et al., 2014; M. Zhang et al., 2012).

In healthy individuals, the reference range for L-Proline levels in the blood has been reported to be 15.8 to 29.1 microgram per milliliter (µg/mL) (S. Liang et al., 2015). However, it's important to note that reference values can vary slightly between different laboratories due to variations in measurement methods and population demographics. These reference ranges serve as a guideline for assessing L-Proline levels in clinical contexts and can help identify potential abnormalities in amino acid metabolism (Mohammad Hasanzadeh et al., 2017; S. Liang et al., 2015; Simonian et al., 1992).

2.3. Molecular Imprinting Technique

Molecular imprinting, a rapidly advancing technology, holds great promise (Verheyen et al., 2011). It involves creating synthetic structures that imitate natural molecular recognition processes (Ramström and Ansell, 1998; Alexander et al., 2006). Molecular recognition happens when two molecules are chemically and geometrically compatible, connected by non-covalent bonds like hydrogen bonds, electrostatic interactions, hydrophobic interactions, weak metal coordination, or by fitting together in size and shape (Ramström and Ansell, 1998; Tsukagoshi, 2001; Bergmann and Peppas, 2008; Hillberg and Tabrizian, 2008).

This natural phenomenon of molecular recognition is widespread in biological processes. Examples include enzyme-substrate binding, virus entry into cells via receptors, antigen-antibody recognition in the immune system, drug interaction with biological targets, messenger RNA formation from DNA templates, odor molecule binding to nasal cavity olfactory receptors, and neuronal signal transduction (Tsukagoshi, 2001; Bergmann and Peppas, 2008; Hillberg and Tabrizian, 2008). Consequently, molecular recognition plays a pivotal role in all life processes (Tsukagoshi, 2001; Bergmann and Peppas, 2008; Hillberg and Tabrizian, 2008).

In biological and chemical processes, especially when similar molecules to the target molecule are present in the environment, there's a need for precise recognition of the target molecule. Molecularly imprinted polymers (MIPs) offer several advantages, including high physical strength, resistance to high temperature and pressure, stability against acids, bases, metal ions, and organic solvents, as well as being cost-effective and easy to prepare. However, traditional MIPs have limitations in some applications, such as inefficient mass transfer and weak zones where molecules can access, along with uneven distribution of binding sites. Moreover, many polymerization methods aren't compatible with water. To address these challenges, the development of a molecular surface printing technique using the sol-gel method has been proposed as an ideal solution (Tsukagoshi, 2001; Tan and Tong, 2007; Hu, 2013).

2.3.1. Synthesis of molecularly imprinted polymers

Molecular imprinting technology (MIT) relies on creating specific recognition spaces within a polymer structure that retains the memory of a template molecule. This results in the formation of a polymeric material known as a "molecularly imprinted polymer (MIP)," which can bind selectively to the target molecule of interest (Alexander et al., 2006; L. Chen et al., 2011; Zenger & Peşint, 2022). These recognition sites are crafted around the target molecule through the polymerization of cross-linkers and functional monomers. Once the polymerization is complete, the template molecule is removed from the resulting polymer, leaving behind binding sites that match the target molecule in terms of size, shape, and the arrangement of functional groups (Alexander et al., 2006; Singabraya et al., 2012; Zenger & Peşint, 2022).

The process of MIT primarily involves the following three steps:

1. Creating a pre-complex composed of the target molecule (template) and a suitable ligand (functional monomer).
2. Polymerizing cross-linkers and primary monomers around the pre-complex.
3. Eliminating the template molecule from the polymeric system to generate specific binding cavities that precisely complement the template molecule in size, shape, and the arrangement of functional groups (Arshady & Mosbach, 1981).

Consequently, this imprinting process leaves behind a molecular recognition memory within the polymeric material, allowing it to selectively rebind the template molecule (Alexander et al., 2006; Andersson, 2000; Martín-Esteban, 2013).

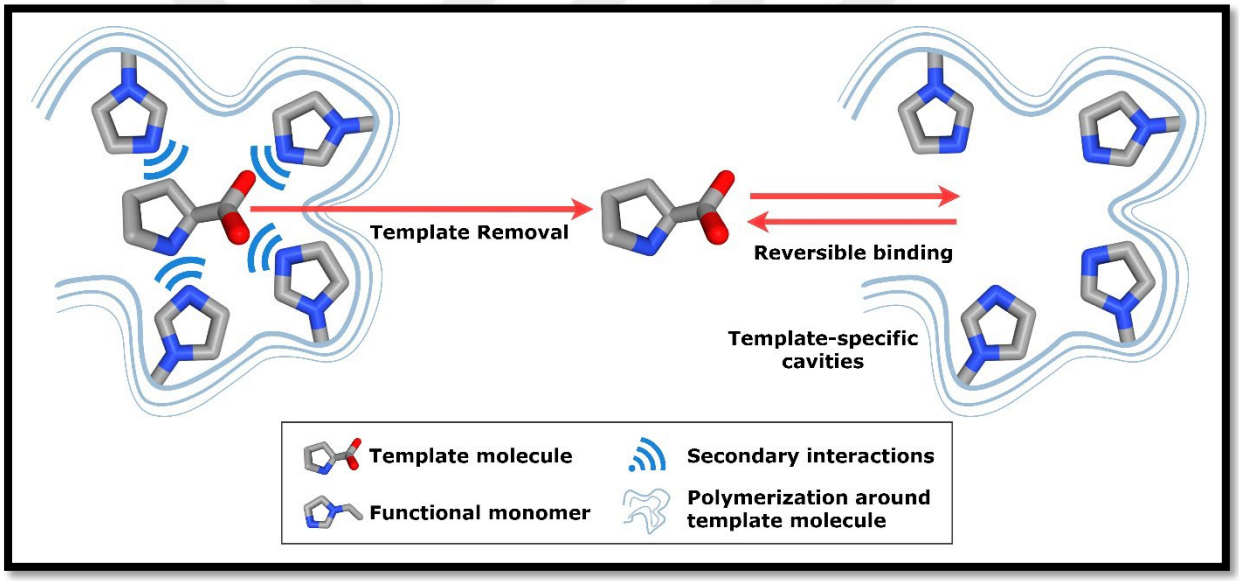

Figure 2.5. Representative illustration of molecular imprinting technique: pre-complexation, polymerization around pre-complex, removal of the template molecule and formation of template-specific cavities.

In comparison to alternative recognition systems, MIPs exhibit notable advantages, including straightforward preparation, high stability, and the ability to be reused under challenging chemical and physical conditions. These attributes have made MIPs increasingly appealing in various applications, particularly in selective solid-phase extraction, chromatographic

separation, and chemical sensors (Alexander et al., 2006; Andaç et al., 2012; L. Chen et al., 2011; Martín-Esteban, 2013). MIPs can be synthesized using three fundamental approaches: non-covalent imprinting, covalent imprinting, and semi-covalent imprinting.

Non-covalent imprinting, widely employed due to its simplicity, involves mixing suitable monomers with the template molecule in a porogen during synthesis. Afterward, the template molecule is easily removed by washing with an elution agent, maintaining the polymer's structure. Adsorption of the template molecule to the MIP occurs through non-covalent interactions like ionic, hydrophobic, and hydrogen bonds. Hydrogen bonds, particularly involving functional monomers like acrylic acid and methacrylic acid, are often the chosen recognition interactions (Arshady & Mosbach, 1981). To eliminate non-covalent interactions, treatment with aqueous solutions of acids, bases, or alcohol is effective, allowing the removal of template molecules from the polymer network post-polymerization. This approach offers quick and reversible binding of the template molecule and is versatile across various templates (Arshady & Mosbach, 1981; Yan & Row, 2006). However, the thermodynamic control of template binding to functional monomers in non-covalent imprinting may lead to inadequate and non-specific binding sites. The variable strengths of non-covalent interactions contribute to heterogeneous binding sites, thereby impacting rebinding activity (Alexander et al., 2006; Arshady & Mosbach, 1981).

Covalent imprinting involves the formation of covalent bonds between the template molecule and the functional monomer before polymerization. Following synthesis, these bonds are broken chemically to detach the template molecule from the polymer matrix (Hansen, 2007; Wulff, 1993; Wulff & Knorr, 2001). Monomers such as boronic acid esters, ketals, disulfide bonds, acetals, and Schiff bases are utilized in this method (Bergmann & Peppas, 2008). Covalent imprinting ensures a more homogeneous distribution of binding sites due to the high stability of covalent bonds. However, the selection of template molecules for covalent imprinting is limited, requiring rapid and reversible covalent bonds between the functional monomer and the template. Slow binding and dissociation, attributed to strong covalent bonds, make achieving thermodynamic equilibrium challenging (Hansen, 2007; Merdas, 2021). Kinetically controlled binding of the template to functional monomers in this approach

decreases the rate of template rebinding upon cavity re-occupation. The combination of the preparation technique and template size/shape may lead to diffusion problems, resulting in reduced rebinding activity (Alexander et al., 2006).

Semi-covalent imprinting arises from the amalgamation of covalent and non-covalent imprinting methods. In this strategy, a covalent bond forms between the template molecule and the functional monomers before polymerization. Following the removal of the template molecule from the polymer matrix, reattachment of the analyte to the Molecularly Imprinted Polymer (MIP) occurs through non-covalent interactions, akin to the non-covalent suppression protocol (Hansen, 2007). The semi-covalent approach provides advantages, including the establishment of homogeneous binding sites through covalent imprinting and swift, reversible adsorption through non-covalent imprinting (Tan & Tong, 2007).

2.3.2. Synthesis conditions

The polymerization reaction is influenced by various factors, including temperature, reaction time, polymeric solution volume, solvent (porogen), and the application of a magnetic field. Additionally, the concentration and type of key components—template molecule, monomer, cross-linker, initiator—and the size of the template molecule play crucial roles. Optimization of reaction conditions is essential to achieve an ideal polymer, tailored to the intended purpose (Alexander et al., 2006; Öncel et al., 2017; Wulff, 1995; Yan & Row, 2006).

2.3.2.1. Template molecule

In most analytical procedures, target compounds serve as template molecules in molecular imprinting, which can include inorganic or organic molecules as well as biomacromolecules. An ideal template molecule should lack functional groups that might disrupt the polymerization reaction, potentially leading to incomplete polymerization. The chemical stability and conformational integrity of the template molecule are critical in the molecular imprinting process. Template molecules with low chemical stability may undergo undesirable changes in both chemical composition and geometry under harsh reaction conditions, compromising the intended outcome. Imprinting proteins poses challenges due to their highly flexible conformation, complex surface structures, and diverse sequences, often resulting in the

formation of non-specific binding cavities that the template molecule cannot effectively bind to or fit into (L. Chen et al., 2011; Dainiak et al., 2007). Consideration of the size of the molecule of interest is crucial. In Molecular Imprinting Technology (MIT), imprinting large templates like proteins, virus particles, or bacterial cells is a complex process. The large structures of biological macromolecules limit movement within the cross-linked polymer network, reducing reattachment efficiency. Consequently, modifications to reaction conditions, reagents, and overall procedures are necessary, tailored to the specific nature of the template (L. Chen et al., 2011; Dainiak et al., 2007; Ertürk & Mattiasson, 2017).

2.3.2.2. Monomers

The monomer assumes the role of introducing functional groups capable of forming a complex with the template molecule through covalent or non-covalent interactions. The strength of interactions between the monomer and the template molecule directly influences the affinity of Molecularly Imprinted Polymers (MIPs) and the selectivity of their recognition sites. A more robust interaction yields a more stable complex and enhances the binding capacity of MIPs, underscoring the significance of judiciously selecting functional monomers. This selection process typically involves challenging trial and error tests. Various techniques, including spectroscopic measurements (nuclear magnetic resonance, UV-vis, Fourier-transform infrared spectroscopy, etc.), computer simulation, and isothermal titration calorimetry, are employed to identify the most suitable functional monomer capable of forming a stable complex with the template molecule (Vasapollo et al., 2011; Zink et al., 2018).

Monomers such as Methacrylic acid (MAA), Glycidylmethacrylate (GMA), Acrylic acid (AA), 2- or 4-Vinylpyridine (2- or 4-VP), Acrylamide, Trifluoromethacrylic acid (TFM), and 2-Hydroxyethylmethacrylate (HEMA) find widespread use in Molecular Imprinting Technology (MIT), as illustrated in Figure 2.6. During synthesis, the molar ratio between the monomer and the template molecule plays a critical role in imprinting efficiency and MIP affinity. Low molar ratios result in fewer binding sites due to a reduced template-monomer complex, while relatively high molar ratios increase non-specific binding capacity but diminish binding selectivity. Thus, optimizing the template-to-monomer molar ratio is essential for achieving high imprinting efficiency. Functional monomers must possess compatible functional groups

to interact with the template molecule (Öncel et al., 2017; Vasapollo et al., 2011; Yan & Row, 2006).

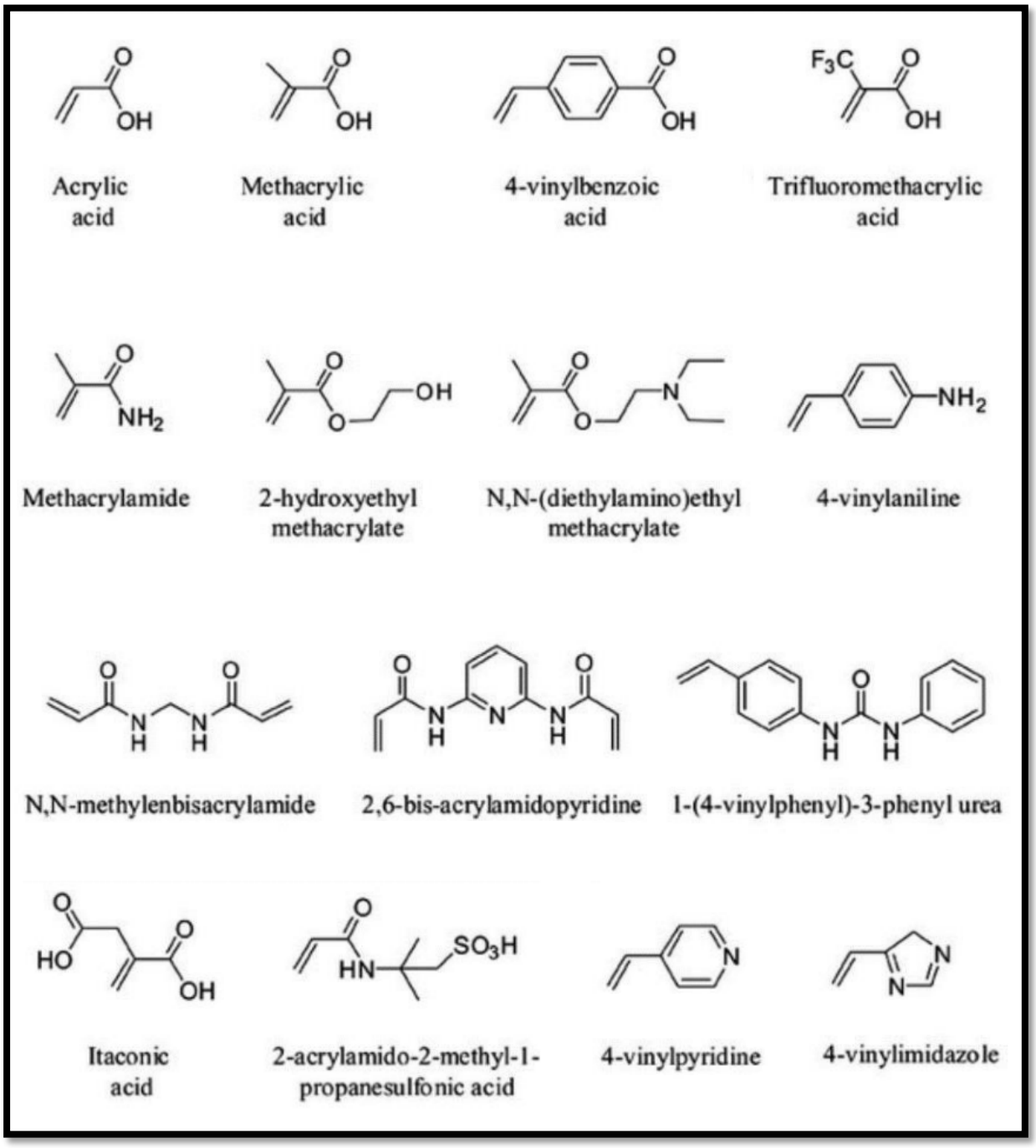

Figure 2.6. Commonly used functional monomers in molecular imprinting.

2.3.2.3. Cross-linker

The cross-linker functions as a bridge between monomer functional groups, facilitating the creation of a highly cross-linked polymeric matrix around imprinted molecules. The polymer's selective binding properties and capacity are significantly influenced by the type and concentration of the cross-linker. Inadequate cross-linker concentration leads to insufficient cross-linking, resulting in MIPs lacking stability gap configurations. Conversely, a relatively higher cross-linker concentration reduces specific binding sites per unit mass of MIPs due to non-covalent interactions and increased heterogeneous copolymerization. A diverse range of cross-linkers, including Ethylene Glycol Methacrylate (EGDMA), Trimethylolpropane Trimethacrylate (TRIM), N,N-Methylenebisacrylamide (MBAA), Divinylbenzene (DVB), and Pentaerythritol Triacrylate (PETA), is employed in Molecular Imprinting Technology (MIT) studies, as depicted in Figure 2.7. Cross-linkers play a crucial role in maintaining the conformational stability of recognition cavities and the overall morphology of MIPs. Essentially, the cross-linker acts as the structural framework in the polymeric material (Alexander et al., 2006; Öncel et al., 2017; Vasapollo et al., 2011).

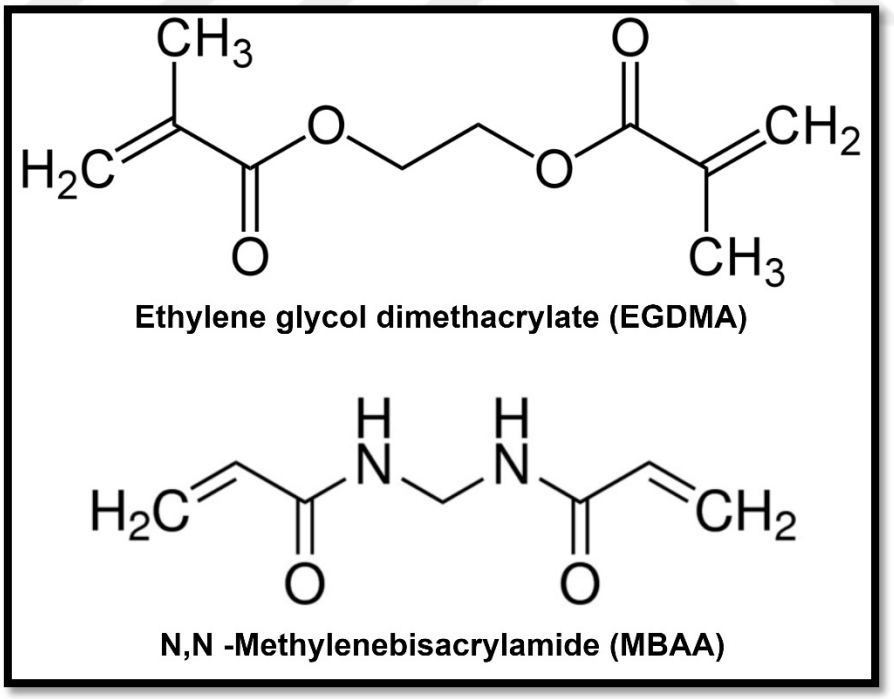

Figure 2.7. Commonly used cross-linkers in molecular imprinting.

2.3.2.4. Solvent

The solvent in a polymeric solution functions as a porogen, playing a vital role in the synthesis of MIPs and influencing the polymerization process. In the non-covalent interaction system, the solvent significantly impacts the structure and size of micro- and macropores, as well as the morphology, swelling capability, mechanical strength, and binding properties of the polymer. Maintaining a balance in the amount of solvent is crucial, and optimization based on the template molecule's size is necessary(Alexander et al., 2006; Vasapollo et al., 2011; Yan & Row, 2006). Aprotic and low-polarity organic solvents like toluene, acetonitrile, and chloroform are commonly used in non-covalent polymerization processes for their role in ensuring excellent imprinting efficiency. Additionally, the innovative use of ultrapure water (UW) as a porogen has gained attention due to the biocompatibility of MIPs (L. Chen et al., 2011).

2.3.2.5. Initiator/Catalyst System

Polymerization reactions requires an initiator/catalyst system to stimulate free radical formation, initiating the polymerization process. Well-established initiators include benzoyl peroxide, lauryl peroxide, ammonium peroxide, azobisisobutyronitrile (AIBN), potassium persulfate (KPS), ammonium persulfate (APS), etc. which can be employed independently or, more commonly, in conjunction with the catalyst such as N,N,N’,N’-tetramethylenediamine (TEMED). The initiator/catalyst system facilitates rapid polymerization, commencing within seconds after its introduction into a monomer solution (Alexander et al., 2006; Yan & Row, 2006; Zenger & Peşint, 2022).

2.4. Nanotechnology

Nanotechnology is an interdisciplinary arena that involves manipulating matter at the atomic and molecular scale. It grapples with materials and devices that possess at least one dimension in the nanometer range, usually between 1 and 100 nanometers (Drexler, 2004). At the nanoscale, materials can showcase exceptional properties and behaviors owing to quantum effects and augmented surface area-to-volume ratio. Nanotechnology concentrates on

comprehending and regulating these properties to form new materials, devices, and systems with advanced or unfamiliar functionalities (Khan et al., 2022).

Nanotechnology encompasses a vast array of scientific disciplines, comprising physics, chemistry, materials science, biology, and engineering. It entails devising, synthesizing, characterizing, and applying nanoscale materials, structures, and devices (Bayda et al., 2019). Nanotechnology boasts the ability to tinker with and engineer materials at the atomic and molecular levels. Scientists can construct nanoparticles, nanotubes, and nanowires with exacting precision over their dimensions, forms, compositions, and surface features.3 These crafted nanomaterials possess diverse electrical, optical, magnetic, mechanical, and chemical properties that contrast starkly with their bulk equivalents (Bayda et al., 2019; Drexler, 2004).

Nanotechnology harbors boundless potential for diverse applications, spanning domains such as electronics, medicine, energy, environmental science, materials science, and many others. By exploiting the distinct attributes of nanoscale materials, researchers and engineers can fabricate smaller, swifter, and more efficient technologies, devise targeted drug delivery systems, devise lightweight but durable materials, and enhance energy production and storage. These are just a few of the surging innovations enabled by nanotechnology (Bayda et al., 2019; Drexler, 2004; Sim & Wong, 2021; Song et al., 2022). In summary, nanotechnology proffers thrilling prospects for groundbreaking innovation and discovery by exploring and manipulating matter at the nanoscale, thereby unlocking fresh frontiers in science, engineering, and technology. This cutting-edge technology allows for the alteration of material properties to improve their functionality (Maynard, 2007). Its numerous applications are exemplified by the following instances:

Electronics: Nanotechnology has the potential to miniaturize electronic components, enhance their speed and energy efficiency. Nanomaterials can be incorporated into transistors, sensors, and memory devices to improve performance (Song et al., 2022).

Medicine and Healthcare: Nanotechnology has revolutionized drug delivery, medical imaging, and biosensors. Its potential applications extend to cancer treatment, infection control, and tissue engineering (Sim & Wong, 2021; Wong et al., 2013).

Energy: Nanotechnology has enabled breakthroughs in energy production and storage. Through the use of nanomaterials, solar cells, fuel cells, and energy storage systems can be made more efficient, cheaper, and sustainable (Abdalla et al., 2020).

Materials Science: Nanotechnology has opened up new avenues in material science, where physical and chemical properties of nanomaterials are harnessed to produce improved materials. Applications include the development of lighter, stronger, and more flexible materials, water-resistant coatings, and pollution reduction (Malik et al., 2023).

Environment: Nanotechnology presents a promising solution to environmental challenges such as water purification, air quality improvement, waste management, and eco-friendly manufacturing processes. Nanomaterials can mitigate environmental impacts and promote sustainability (Coşkun et al., 2017).

Food and Agriculture: Nanotechnology offers revolutionary possibilities in food processing, packaging, and storage. Nanomaterials can enhance the barrier properties of food packaging, extend the shelf life of food items, and control plant diseases, improve fertilizer efficiency, and enhance plant growth in agriculture (Wong et al., 2013).

2.4.1. Nanobiotechnology

Nanobiotechnology is the union of nanotechnology and biotechnology, where nanomaterials and nanotechnological approaches interact with biological systems. This cutting-edge field has boundless potential applications, such as medicine, drug discovery, diagnostic methodologies, biosensors, and biomaterials (Su & M Kang, 2020). Here are some examples of how nanobiotechnology can change the game:

Drug Delivery Systems: Nanobiotechnology enables the development of super-small carriers, which can transport drugs to the desired location with greater precision and safety, minimizing any side effects (Shoaib et al., 2023).

Biosensors: Using nanomaterials, ultra-sensitive and accurate biosensors can be produced. These can be utilized in medical diagnostics, like monitoring blood sugar levels, detecting infections, and screening for cancer, as well as in environmental analysis (Nagamune, 2017).

Biomolecular Imaging: Nanobiotechnology provides advanced imaging techniques to visualize biomolecular structures. By labeling molecules with nanomaterials, intracellular events and protein interactions can be visualized with ease (Kushwaha et al., 2022).

Biomaterials: Nanomaterials can enhance biomedical biomaterials. For example, nanoparticles can accelerate wound healing and improve the properties of biomaterials used in tissue regeneration (Shahcheraghi et al., 2022).

Biotechnological Production: Nanobiotechnology can improve biotechnological production processes through nano-scale reactors and nanomaterials. This can lead to more efficient and cost-effective manufacturing methods (Thwala et al., 2023).

Molecular Diagnostics: Nanobiotechnology can advance molecular diagnostic methods. For instance, nanotechnology-based polymerase chain reaction (PCR) techniques can speed up and increase the precision of genetic analysis (Santos et al., 2015).

2.4.2. Nanoparticles

Nanotechnology, in general, refers to materials with dimensions smaller than 100 nm at the nanoscale. The chemical properties of nanomaterials in the range of 1-100 nm significantly differ from those of micro and macro-scale materials (Ameen et al., 2021). Nanomaterials have garnered great interest in scientific research due to their versatile chemical properties, such as

high chemical and physical stability, functionalizability, and unique characteristics like high surface area (Hulkoti & Taranath, 2014).

Nanoparticles are intriguing nano-scale systems that can be easily produced in various forms. The exceptional chemical properties of nanoparticles vary depending on their small size (<100 nm), surface area and structure, surface reactivity, surface-bound functional groups and coatings, chemical composition, crystallinity and electronic properties, solubility, shape, clustering behavior, and surface charges (Mauter et al., 2018). The inherent characteristics of nanoparticles, their behavior in different environments, and their distinguishing features arise from their higher surface energy compared to bulk materials (Hulkoti & Taranath, 2014).

One of the unique features of nanoparticles is their high surface area-to-volume ratio, which provides them with high reactivity and physicochemical dynamics (Behzad et al., 2021). Due to their distinctive properties, nanoparticles play a significant role in engineering, medicine, and pharmacology. They are widely used in industrial, biomedical, and technological applications, particularly in sectors such as cosmetics, food, textiles, electronics, aerospace industry, medicine, and biotechnology (Kolahalam et al., 2019).

Nanoparticles come in different types and can be categorized based on their shapes, sizes, chemical and physical properties, and components. Commonly used nanoparticles include metal nanoparticles, metal oxide nanoparticles, carbon-based nanoparticles, semiconductor nanoparticles, polymeric nanoparticles, and lipid-based nanoparticles (Paksoy et al., 2022).

2.4.2.1. Nanoparticle preparation methods

Various processes, encompassing physical, chemical, and biological methods, are employed in the production of nanoparticles. These processes can be broadly classified as either bottom-up or top-down techniques (Dhand et al., 2015; Ramanathan et al., 2021). The conditions under which synthesis occurs play a pivotal role in determining the fundamental properties of NPs. These properties encompass factors such as size and size distribution, crystalline structure, morphology, and directional attributes (Sajid & Płotka-Wasylka, 2020).

Bottom-up and top-down approaches are two distinct methods for synthesizing nanoparticles, each with its own principles and techniques. The bottom-up approach, also known as the "nanosynthesis" or "chemical synthesis" approach, starts with atomic or molecular constituents and builds up to form nanoparticles through chemical reactions or self-assembly processes. Various techniques fall under the bottom-up category, including:

- *Chemical Reduction:* Precursor materials are reduced to form nanoparticles in the presence of reducing agents.
- *Sol-Gel Method:* Nanoparticles are formed by the gradual conversion of a sol (solution) into a gel and then into a solid material.
- *Self-Assembly:* Molecules or atoms arrange themselves into nanoparticles through natural affinity or manipulation.
- *Biosynthesis:* Biological organisms, such as bacteria or plants, are used to synthesize nanoparticles.

Bottom-up methods allow precise control over the size, shape, and composition of nanoparticles. They are well-suited for creating complex nanostructures and functionalizing nanoparticles for specific applications (Dhand et al., 2015; Ramanathan et al., 2021).

The top-down approach involves the reduction of larger materials or structures, typically at the macroscopic scale, into nanoparticles by breaking them down into smaller fragments. Various techniques fall under the top-down category, including:

- Milling: Larger materials are ground into smaller particles using mechanical forces.
- Lithography: Photolithography or electron beam lithography techniques are used to create patterns on a material's surface, which is then etched to form nanoparticles.
- Chemical Etching: Chemical agents are used to selectively remove parts of a material, leaving behind nanoparticles.
- Vapor Deposition: Material is vaporized and condensed to form nanoparticles on a substrate.

Top-down methods are useful when dealing with bulk materials or when precise control over size and shape is not as critical. They are often employed in the semiconductor industry and for producing nanoparticles from existing materials (Dhand et al., 2015; Ramanathan et al., 2021).

The bottom-up approach starts from the molecular or atomic level and assembles nanoparticles, providing precise control over their characteristics. On the other hand, the top-down approach begins with larger materials and reduces them to nanoparticles, making it suitable for scaling down existing structures but with potentially less control over nanoparticle properties. The choice between these approaches depends on the specific requirements of the nanoparticle synthesis and the desired characteristics of the final nanoparticles (Dhand et al., 2015; Ramanathan et al., 2021).

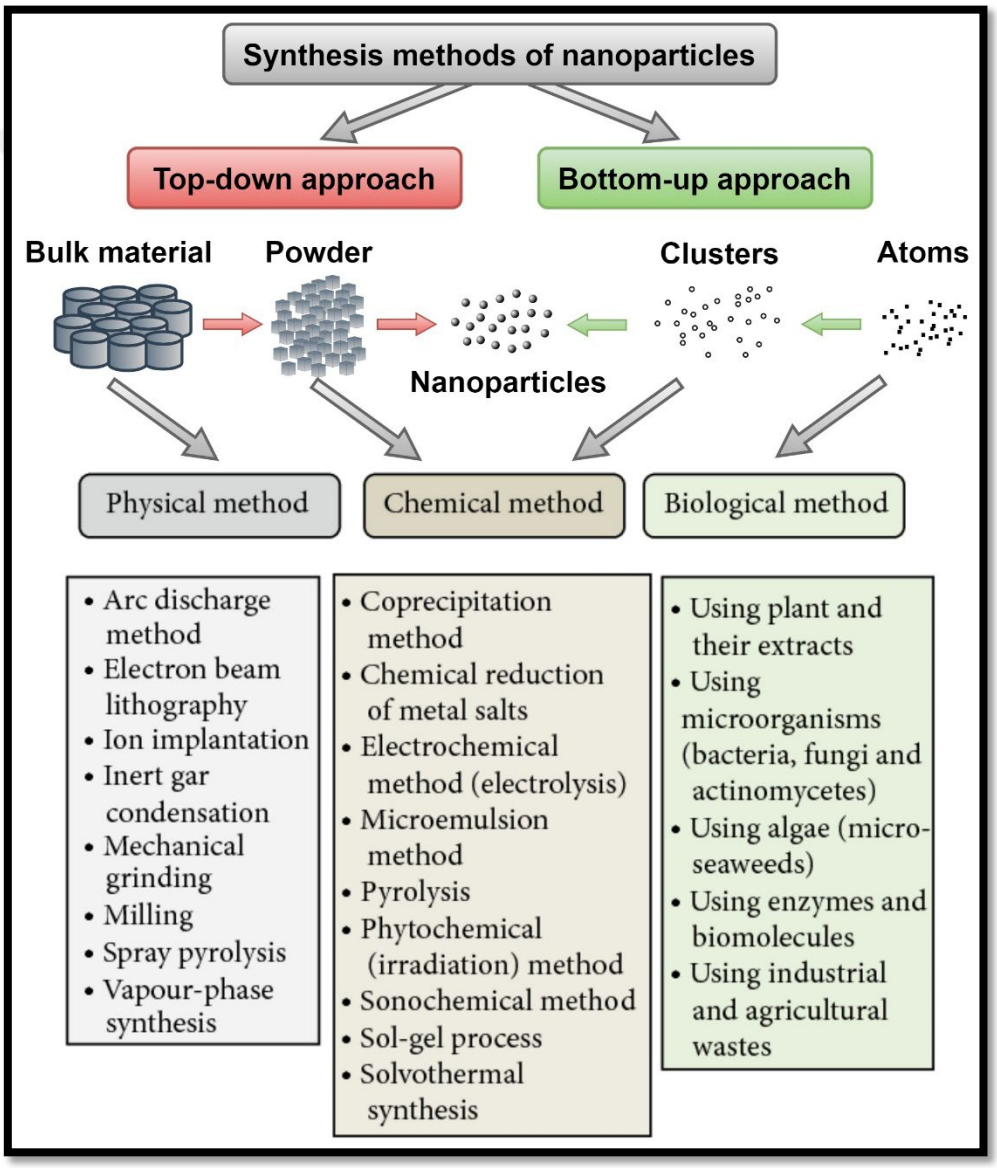

Figure 2.8. Schematic representation of various nanoparticle preparation methods, illustrating the diverse techniques employed in the synthesis of nanoparticles.

Polymerization methods used in nanoparticle synthesis are given below:

- *Suspension Polymerization:* This method involves dispersing monomers in a continuous phase and initiating polymerization to form polymer nanoparticles suspended in the medium.
- *Miniemulsion Polymerization:* It's similar to suspension polymerization but employs smaller droplets, resulting in smaller nanoparticles.
- *Emulsion Polymerization:* Monomers are emulsified into small droplets in an aqueous phase, and polymerization occurs within these droplets to form polymer nanoparticles (Dhand et al., 2015; Ramanathan et al., 2021).

In this thesis study, emulsion polymerization technique was employed for the synthesis of nanoparticles.

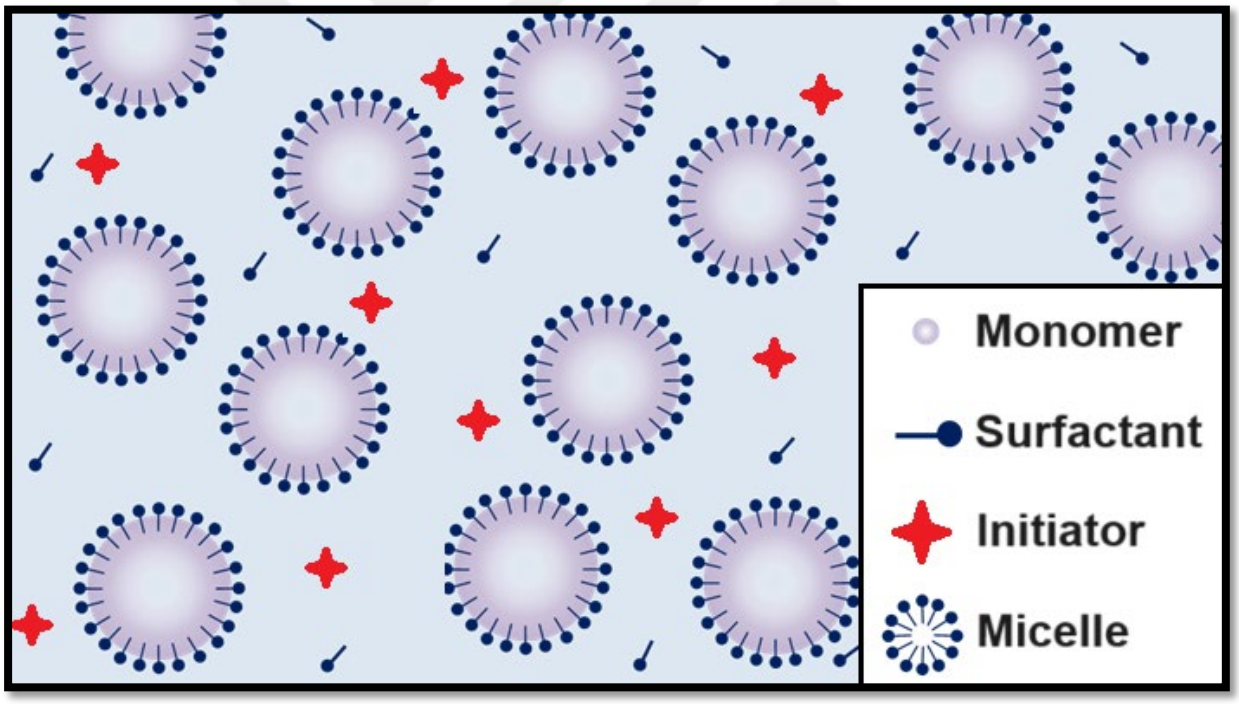

Figure 2.9. Schematic Representation of Emulsion Polymerization: A visual representation highlighting the interplay of monomers, surfactants, and initiators in the emulsion polymerization process.

3. MATERIALS AND METHODS

3.1. Materials

All the chemicals needed for this thesis study, i.e. L-Proline, L-Histidine, L-Phenylalanine, 1-Vinylimidazole (VIM), Ethylene Glycol Dimethacrylate (EGDMA), poly(vinyl alcohol) (PVA), sodium dodecyl sulfate (SDS), 2-hydroxyethyl methacrylate (HEMA), Sodium bicarbonate, ammonium persulfate (APS), Phosphate Buffer Saline (PBS), and ethanol were purchased from Sigma-Aldrich (St. Louis, MO, USA). The required solutions were prepared using Type 1 ultrapure water (UW) with a conductivity of 18 MΩ-cm at room temperature and analytical-grade reagents. Storage guidelines were followed for all reagents, and waste materials were disposed of according to regulations. All chemicals used in our experiments meet reagent-grade purity standards.

In relation to the experimental tools and devices, a Glass polymerization reactor (Radleys Carousel 6 Plus Reaction Station), Homogenizer (BIOBASE D-160, Shandong, China), Centrifuge (Allegra X-30R, Beckman Coulter, USA), Shimadzu Type ATX224 No. D307039788 Electronic Balance, Scientific Vortex Mixer (Daihan, Korea), The GENESYS 150 UV-Vis Spectrophotometer (Thermo Fisher Scientific, USA), Oven (MIPROLAB MLF 120, TURKEY), Model of Millipore DIRECT-Q®3 ultrapure (type 1) water with BioPak® ultrafiltration cartridge with Millipak®Express 20 (0.22 μm) membrane filter, Scanning Electron Microscope (SEM) (FEI, Quanta 650 Field Emission SEM, USA), Zetasizer (Nano S-90, Malvern Instruments, London, UK), FTIR (Fourier Transform Infrared) spectrometer (Jasco FT/IR-6700, Japan), and Hitachi HT-7700, Japan were employed. It is important to note that basic laboratory equipment and consumables are not included in this list.

3.2. Methods

3.2.1. Synthesis of L-proline imprinted and non-imprinted pHEMA based nanoparticles (Pro-MIPs and NIPs)

L-Proline-imprinted and non-imprinted pHEMA based nanoparticles were synthesized through emulsion polymerization of separately prepared aqueous and organic phases. Before the

synthesis, the ideal molar ratio of the template molecule and functional monomer must be determined. For this purpose, spectrophotometric analyses were conducted on different molar ratios of vinyl imidazole to L-Proline (1:1, 1:2, 1:3, 1:4 and 1:5, n:n), keeping mole of L-Proline constant. For the aqueous phase, 575 mg of polyvinyl alcohol (PVA), 257 mg of sodium dodecyl sulfate (SDS), and 47 mg of sodium carbonate were dissolved in 420 mL of ultrapure water. For the organic phase, functional monomer (VIM) and the template molecule (L-proline) were initially mixed at the determined ideal molar ratio to form a pre-complex. This mixture was kept at +4 °C for 4 hours to facilitate complexation. Subsequently, a mixture of 1 mL of hydroxyethyl methacrylate (HEMA) and 4 mL of ethylene glycol dimethacrylate (EGDMA) was combined with the pre-complex. The aqueous and organic phases were mixed in a 500 mL beaker, and the resulting mixture was homogenized at 30,000 rpm for 30 min using a homogenizer to obtain a miniemulsion. Subsequently, the total mixture was taken into the glass polymerization reactor, where it underwent heating at 40°C while being stirred at 300 rpm. Finally, the initiation of the reaction was facilitated by the addition of sodium bisulfite (50 mg) and ammonium persulfate (75 mg) to the mixture. As a control group, non-imprinted nanoparticles (NIPs) were synthesized using the same recipe except for the L-proline:VIM pre-complex. The liquid phase 1, emulsified on a smaller scale, was gradually introduced into the organic phase. The mixture was homogenized at 30,000 rpm for 20 minutes to achieve a miniemulsion. Subsequently, the resulting miniemulsion was then combined with liquid phase 2 and further mixing were performed at 300 rpm using a magnetic stirrer was carried out for an additional 10 minutes. The final mixture was transferred to the glass polymerization reactor, which was heated to 40°C with stirring at 300 rpm. To initiate the reaction, sodium bisulfite (50 mg) and ammonium persulfate (75 mg) were added. Polymerization continued for 24 hours at 40°C.

The synthesized nanoparticles were separated through centrifugation at 18,000 rpm for 50 minutes. The resulting pellets underwent multiple washing steps with ultrapure water (UW) using a rotator to remove any remaining monomers, surfactants, and impurities. Following each washing cycle, the nanoparticle solution was centrifuged at 18,000 rpm for 50 minutes, and the supernatant was carefully removed with a micropipette. Fresh UW was added to the nanoparticles after each cycle. After each washing step, the absorbance of the süpernatant was

measured using a spectrophotometer, and the washing cycles were repeated until the absorbance value reached zero.

3.2.2. Template Removal

After the completion of the washing process to generate L-Proline-specific cavities by eliminating the template molecule from the synthesized Pro-MIPs, nanoparticles were subjected to a 40% ethanol (EtOH) elution agent in a batch system using a rotator. In this process, 50 mL of the elution solution was introduced to the nanoparticles, leading to their dissolution and dispersion in the elution solution via an ultrasonic water bath for 15 minutes. Subsequently, Pro-MIPs were exposed to 40% EtOH in the rotator for 2 hours, followed by centrifugation at 18,000 rpm for 50 minutes. The resulting supernatant was measured at 520 nm using ninhydrin reagent which was used for monitoring L-proline leakage spectrophotometrically. The template removal step was repeated until no L-Proline molecule was detectable in the supernatant.

L-Prolin measurement using the Ninhydrin method: For the reaction mixture, Ninhydrin (1% by weight) was dissolved in 60% acetic acid prepared in 20% ethanol. For measurement, 1 mL of the reaction mixture, 100 µL of the sample containing proline, and 500 µL of ethanol (40:60, v:v) were mixed and incubated at 95°C in a water bath for 20 minutes. After incubation, the samples were measured at 520 nm using a UV spectrophotometer (Kijowska-Oberc et al., 2020).

Amount of removed L-Proline (Q_{tr}) and template removal ratio (%) were calculated using following equations (Zenger & Peşint, 2022):

$$Q_{tr} = C_{Pro} \times (V/m_{dry}) \quad (1)$$

$$TR\ (\%) = (Q_{tr}/ Q_i) \times 100 \quad (2)$$

Here, C_{Pro} is L-proline concentration in elution medium in mg/mL, V is the volume of elution agent in mL and m_{dry} is the dry weight of the Pro-MIPs in g. Q_{tr} is L-Proline removal amount (mg/g) and Q_i is the amount of L-proline in polymerization feed (mg/g).

3.2.3. Characterization Studies

The calculation of nanoparticle polymerization yield involved assessing the polymerization feed amounts and the dry weight of the particles. To calculate the surface area of the nanoparticles, the density of the polymer and dimensional analysis results were utilized. Characterization of the prepared nanoparticles involved Zeta-Sizer Analysis, Scanning Electron Microscopy (SEM), Transmission Electron Microscope (TEM), and FTIR spectrophotometer. The zeta-sizer device was employed to measure the sizes and size distribution of the nanoparticles. FTIR spectrophotometer analysis was used for a comparative examination of the chemical structures of L-Proline, VIM, L-Proline:VIM pre-complex, Pro-MIPs, and NIPs. SEM analysis captured large-scale images of the nanoparticles, showing their particle sizes and morphological structures.

3.2.3.1. Polymerization efficiency

To determine the polymerization efficiency of the synthesized nanoparticles, the first step involved swelling the nanoparticle samples in 250 µL of ultrapure water (UW) and freezing them at -16 °C. Subsequently, the samples were lyophilized at 0.001 mbar and -50 °C for a duration of 8 hours to obtain their dry weight. The polymerization efficiency was then calculated using the following equation (Yıldırım & Baydemir Peşint, 2021):

$$\text{Polymerization Efficiency (\%)} = (m_{dry}/m_t) \times 100 \quad (3)$$

Here, m_t represents the total mass of the monomers in the feed polymer mixture.

3.2.3.2. Nanoparticle size analysis

Size analysis of Pro-MIPs and NIPs was conducted using the Zetasizer Nano S-90 (Malvern Instruments, London, UK) at the Nanotechnology Application and Research Laboratory, Adana Alparslan Türkeş Science and Technology University. The Zetasizer device employs a light scattering technique for nanoparticle size measurement. The particle size analysis proceeded as follows: Nanoparticles were dissolved in water, ensuring complete dissolution and preventing any accumulation or aggregation of particles using an ultrasonic water bath. Subsequently, 1.5

mL of the nanoparticle solution was taken and placed in the cuvette for measurement. Light scattering occurred at an incidence angle of 90° and at a temperature of 25°C. For data analysis, the viscosity and refractive index of deionized water were entered as 0.8822 cP and 1.33, respectively, with the absorption of the polymer set at 0.001. The light scattering signal was calculated as the number of nanoparticles per second, and the instrument confirmed that the nanoparticle concentration in the solution was sufficient for accurate measurement. Each result was averaged by replicating the procedure three times.

3.2.3.3. Scanning Electron Microscopy

The investigation of morphological structures and particle sizes of Pro-MIPs and NIPs was conducted using Scanning Electron Microscopy (FEI, Quanta 650 Field Emission SEM, USA) at Çukurova University Central Research Laboratory. Prior to SEM analysis, Pro-MIP and NIP samples were prepared by being dispersed in an ultrasonic water bath in ethyl alcohol. Subsequently, the fully dissolved and dispersed nanoparticle samples were deposited onto a glass coverslip and allowed to dry in an oven (Miprolab MLF 120, Turkey) at 40°C for 2 hours. After drying, the nanoparticle samples were fixed by being transferred from a glass coverslip onto the SEM sample plate using a conductive adhesive. This step was crucial to ensure that the nanoparticles were affixed as thinly as possible on the SEM sample plate, facilitating optimal imaging. Finally, the samples were sputter-coated with a gold-palladium alloy (40/60) before being examined using a JEOL JSM 5600 scanning electron microscope (Tokyo, Japan). This enhanced methodology was employed to achieve comprehensive and high-quality SEM images.

3.2.3.4. Structural analysis

Fourier Transform Infrared (FTIR) analysis is a fast, non-invasive, and time-efficient method that can identify the functional groups within solid, liquid, or gaseous samples, showing sensitivity to changes in molecular structure. Using the FTIR spectrophotometer, the chemical composition of nanoparticles was examined by comparing the presence of the template molecule and the VIM functional monomer in the structures of Pro-MIPs and NIPs. Notably, Pro-MIPs were solely subjected to washing, skipping the template removal process. For comprehensive structural characterization of samples, i.e. L-Proline, VIM, Pro-VIM pre-

complex (1:4), Pro-MIP, and NIP, the Jasco FT/IR-6700 FTIR spectrometer (Japan) was used at Çukurova University Central Research Laboratory.

Before starting the analysis, nanoparticles were separated from the nanoparticle solution via centrifugation, followed by freezing with retained water, and subsequent freeze-drying, while other samples underwent no additional processes. Spectra were then captured in the wavenumber range of 400-4000 cm^{-1} to provide a detailed understanding of the molecular composition and interactions within the synthesized materials. This diverse approach to FTIR analysis offers valuable insights into the chemical structures of the investigated nanoparticles.

3.2.4. Adsorption Studies

The adsorption characteristics of Pro-MIP and NIP nanoparticles for L-Proline molecule were examined in a batch system using aqueous L-Proline solutions at 25 °C. The study delved into understanding the effect of initial L-Proline concentration (ranging from 0.01 to 1 mg/mL), interaction time (0 to 120 minutes), and temperature (4, 25, 37 ve 45°C) on the L-Proline adsorption onto nanoparticles. Adsorption studies were conducted with PBS, pH 7.0 to ensure physiological conditions.

3.2.4.1. Effect of initial L-proline concentration on adsorption

For investigating the impact of the initial L-Proline concentration on L-Proline adsorption, nanoparticles were taken in equal amounts (60 mg each) into Eppendorf tubes. L-Proline solutions at increasing concentrations (0.01, 0.025, 0.05, 0.1, 0.2, 0.3, 0.45, 0.6, and 1 mg/mL) were added to the nanoparticles within a specified range. The mixture was left to adsorb for 2 hours in a batch system using a rotor. Subsequently, the nanoparticles were centrifuged at 18,000 rpm, and the supernatant was measured using the Ninhydrin method.

Adsorption capacities were calculated using the following equation (Aylaz et al., 2022):

$$Q = (C_i - C_f) * (V/m) \quad (4)$$

Here, Q is the amount of adsorbed L-Proline for the unit mass of nanoparticles (mg/g), C_i is concentration of L-Proline solution before interaction with nanoparticles (mg/mL), C_f is

concentration of L-Proline solution measured after 2h interaction with nanoparticles (mg/mL), V is volume of L-Proline solution (mL), and m is the dry mass of the nanoparticles (g).

The experimental adsorption data were utilized to explore the interaction between nanoparticles and L-Proline molecules through adsorption isotherms. Adsorption isotherms facilitate the understanding of the relationship between the amount of adsorbate adsorbed on the adsorbent (qe) and the equilibrium concentration of the adsorbate in the solution (Ce). In this study, these interactions were examined using the Langmuir and Freundlich adsorption isotherm models.

3.2.4.2. Effect of temperature on adsorption

To understand how temperature influences adsorption, 60 mg of nanoparticles was utilized for each Eppendorf tube. Each tubes were taken into an ambient with various temperatures: 4, 25, 37, and 45°C. Adsorption was carried out in a rotator for 2h, followed by centrifugation at 18,000 rpm for 50 min. Spectrophotometric measurements using the ninhydrin reagent were employed to quantify the adsorption.

3.2.4.3. Effect of interaction time on adsorption

To assess the effect of interaction time on L-Proline adsorption onto Pro-MIPs, 0.36 mg of nanoparticles were placed in a Falcon tube containing 9 mL of L-Proline solution with a concentration of 0.6 mg/mL at 25°C and the mixture was rotated using a rotator. Following that, 1.5 mL samples were collected at 0, 5, 15, 30, 45, 60, 90, and 120 minutes, with each sample undergoing precipitation by centrifugation at 18,000 rpm for 50 minutes. The quantification of adsorption was performed through spectrophotometric measurements using the ninhydrin reagent.

The adsorption mechanism was clarified by using adsorption kinetics models. The experimental data of time-adsorption amounts were subjected to both first and second-order kinetic models to determine the mechanisms governing the adsorption process, such as mass transfer/diffusion or chemical reaction/chemical adsorption. Calculations were conducted for both pseudo-first-order kinetics and pseudo-second-order kinetics, and the suitability of the binding kinetics between L-Proline and Pro-MIPs to these models was evaluated.

3.2.5. Selectivity Studies

The selectivity of Pro-MIPs for L-Proline were investigated against competitors, i.e. L-Histidine and L-Phenylalanine, separately, and also in the complex matrix of human serum spiked with L-Proline, L-Histidine and L-Phenylalanine molecules, in batch system. Obtaining samples were examined through LC-MS/MS analysis in order to validate the selevtivity of Pro-MIPs for L-Proline molecule.

The samples obtained from selectivity studies were analyzed using LC-MS/MS. The analyses were performed on a Thermofisher Scientific Ultimate 3000-TSQ Quantis model LC-MS/MS instrument. The column used for the analysis was hydrophilic interaction liquid chromatography column, with a particle size of 2.6 and dimensions of 150*3 mm. The gradient for the mobile phases A and B lines was employed in the analysis. The mobile phase content for line A consisted of 1.5775 g of ammonium formate powder in 250 mL of ultrapure water and 2500 µL of formic acid. The mobile phase content for line B consisted of 500 mL of acetonitrile (ACN) and 500 µL of formic acid. A gradient was applied with 15% from line A and 85% from line B, allowing a flow rate of 0.250 ml per minute. For the sample preparation for LC-MS/MS analysis; 70 µL of deionized water, along with 70 µL of the sample, calibrator, or control, is pipetted into an Eppendorf tube. The mixture is vortexed, followed by a 15-minute incubation at +4°C. Afterward, the tube is centrifuged at 10,000 rpm for 5 minutes. Subsequently, 100 µL of the supernatant is transferred to a plate and evaporated under nitrogen at 40°C. Then, 50 µL of derivatization reagent (NBS reagent B) is added, and the mixture is incubated in an oven at 60°C for 15 minutes. After another nitrogen evaporation step at 40°C, 100 µL of solvent (NBS reagent C) is added, and the solution is allowed to sit on a shaker for 5 minutes. The sample is transferred to a filtered Eppendorf tube and centrifuged for 1 minute. Finally, the prepared sample in the insert vial is submitted to the instrument. For each molecule in the MS/MS system, the mass number for scanning is specified, referred to as ion transitions.

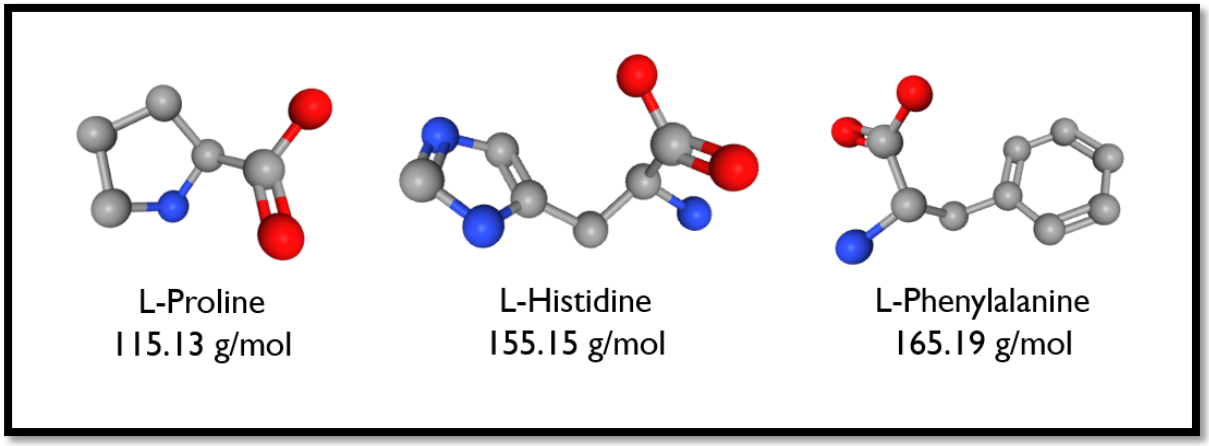

Figure 3.1. Molecular structure of L-Proline and competitor molecules (L-Histidine and L-Phenylalanine).

The amount of adsorbed molecules for each competitors and template was calculated according to following equation, using the data obtained from LC-MS/MS analysis:

$$Q = (C_i - C_f)*(V/m) \quad (5)$$

In this equation, Q represents the adsorption amount (mg/g); C_i and C_f denote the initial and final concentrations of competitors, respectively. V stands for the volume of the solution (mL), and m represents the mass of nanoparticles used (g).

Imprinting factor (IF) for template molecule and competitors were calculated using the following equation, in order to evaluate selective adsorption property of Pro-MIP columns.

$$IF = Q_{Pro\text{-}MIP} / Q_{NIP} \quad (6)$$

In this equation, $Q_{Pro\text{-}MIP}$ and Q_{NIP} represent the adsorption amount (mg/g) onto Pro-MIPs and NIPs, respectively.

The selectivity coefficient for binding of L-Proline in the presence of competitors is obtained from the equilibrium adsorption data according to the following equation:

$k = Q_{template} / Q_{competitor}$ (7)

In this equation, Qtemplate and Qcompetitor stands for the adsorption amount of L-Proline and competitors onto Pro-MIPs, respectively.

3.2.6. Reusability Studies

To test the reusability of the synthesized nanoparticles, repeated adsorption-desorption cycles were performed. The desorption studies of Pro-MIP were carried out in a batch system using 40% EtOH as the desorption solution. Each Eppendorf tube containing 60 mg of Pro-MIP nanoparticles was mixed with 1.5 mL of desorption solution, and rotated using a rotator at 300 rpm for 2 hours at 25 °C. After centrifuging the nanoparticles at 18,000 rpm, the supernatants were collected and analyzed for L-Proline using spectrophotometric measurements with the ninhydrin reagent. The amount of L-Proline in the desorption medium was quantified after each adsorption-desorption cycle. The cycles were repeated until no significant L-Proline leakage was observed in the desorption medium. The desorption rate was calculated using the following equation (Yıldırım & Baydemir Peşint, 2021):

$$Desorption\ Ratio\ (\%) = \frac{The\ amount\ of\ L{-}Proline\ released\ into\ desorption\ medium\ (mg)}{The\ amount\ of\ adsorbed\ L{-}Proline\ (mg)} \text{ x } 100 \quad (8)$$

4. RESULTS AND DISCUSSION

In the course of this thesis study, nanoparticles were synthesized through emulsion polymerization, with a focus on recognizing the L-proline molecule—an important biomarker of various metabolic disorders. Unlike existing literature, molecular imprinting techniques were employed for the direct determination of L-proline in body fluids, presenting a novel approach in the field. The following discussion gives an overview of the synthesis process, highlighting the key analyses conducted, including characterization studies (polymerization yield, approximate surface area, size, and morphology), optimization of experimental conditions via adsorption studies, confirmation of selectivity in complex medium in presence of competitor molecules, and reusability test. This analyses highlight the potential and importance of L-Proline imprinted nanoparticles in advancing diagnostic methodologies for metabolic disorders, particularly in the diagnosis of hyperprolinemia from human serum.

4.1. Synthesis of L-proline imprinted and non-imprinted pHEMA based nanoparticles (Pro-MIPs and NIPs)

Molecularly imprinted HEMA-EGDMA-based nanoparticles were synthesized with high polymerization efficiency in the presence of L-Proline as the template molecule and vinyl imidazole (VIM) as the functional monomer. Prior to the synthesis of L-Proline imprinted nanoparticles, the optimal molar ratio of the template molecule and functional monomer has to be established. To determine the optimum L-Proline:VIM ratio, a spectrophotometric scan was conducted in the range of 450-700 nm by keeping the L-Proline molar ratio constant and increasing the VIM molar ratio, resulting in the graph in Figure 4.1. It was observed that there was no significant alteration in the peak after the 1:4 (Pro-VIM, n:n) molar ratio. Thus, it was decided that the optimal molar ratio for complexation of L-Proline and VIM molecules was 1:4. Therefore, Pro-MIP nanoparticles were synthesized by preparing the Pro-VIM pre-complex at the determined molar ratio. NIP nanoparticles were also successfully synthesized as the control using the same recipe and protocol without the presence of pre-complex.

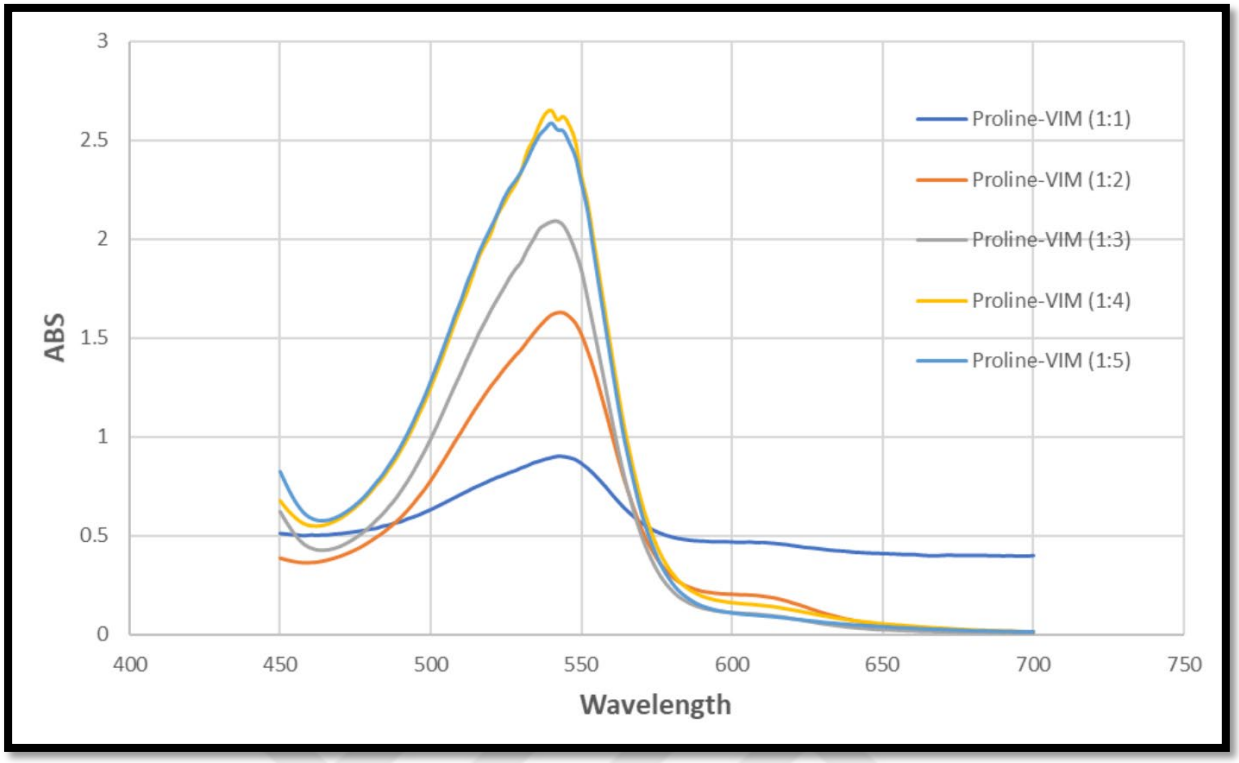

Figure 4.1. Determination of the optimal Pro:VIM molar ratio for complexation. UV-VIS absorption spectra of Pro:VIM (n:n) mixtures prepared in 1:1, 1:2, 1:3, 1:4 and 1:5 ratios.

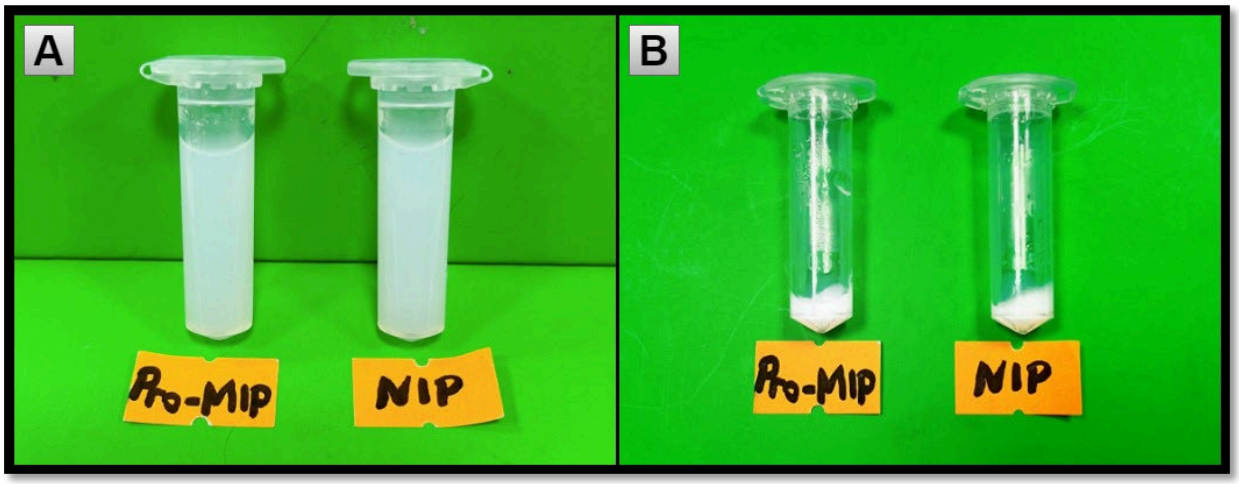

Figure 4.2. Optical photographs of Pro-MIP and NIP nanoparticles A) before centrifuge, B) after centrifuge.

Before starting template removal and adsorption studies, L-Proline solutions at concentrations of 0.01, 0.025, 0.05, 0.1, 0.2, 0.3, 0.45, 0.6, and 1 mg/mL were prepared, and measurements

were taken at 520 nm using the ninhydrin method, spectrophotometrically. The obtained absorbance values were used to generate the calibration curve (R^2: 0.9962) shown in Figure 4.3.

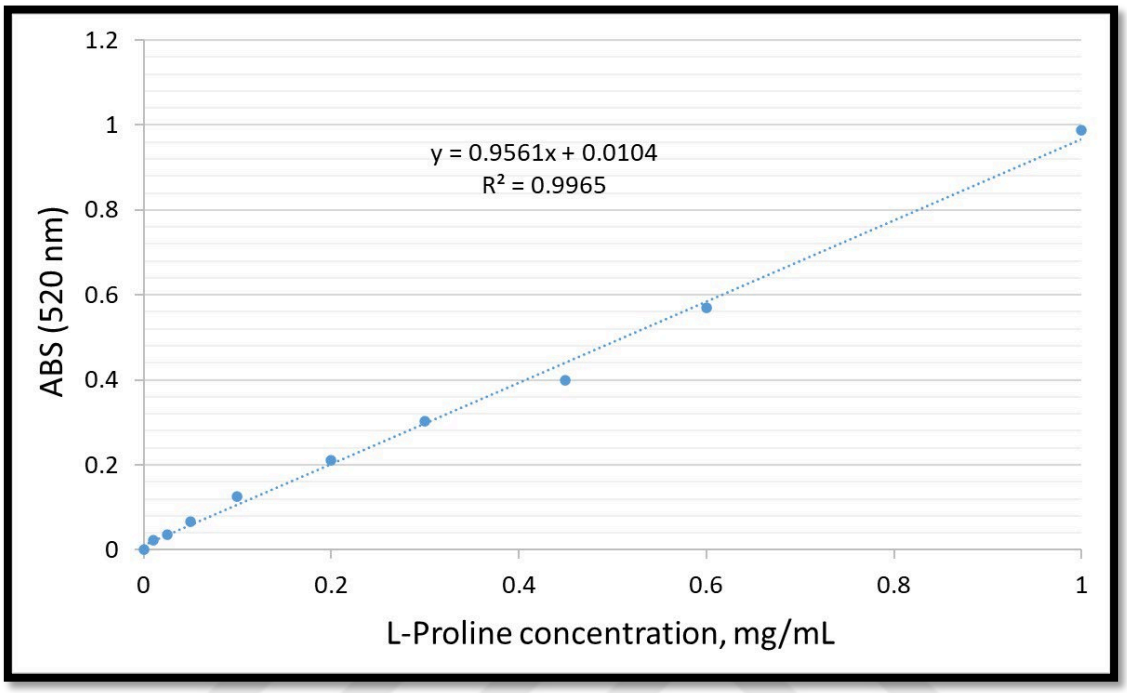

Figure 4.3. Calibration of L-Proline at 520 nm (concentration range: 0.01-1 mg/mL).

4.2. Characterization Studies

Pro-MIP and NIP nanoparticles were well-characterized via polymerization efficiency calculations, zeta-sizer particle size analysis, scanning electron microscopy, surface area measurement and FTIR analysis.

The obtained dry polymer weights were determined as 1.472 grams for Pro-MIPs and 1.508 grams for NIPs. The weights of the substances involved in polymerization were determined as 1.579 grams for Pro-MIPs and 1.533 grams for NIPs. Consequently, according to Equation 3, the polymerization efficiencies of Pro-MIP and NIP nanoparticles were calculated as 93.22% and 98.36%, respectively.

The graphs showing the results obtained from the Zetasizer device are provided below. The average sizes of the synthesized Pro-MIP and NIP nanoparticles were found to be 27.51 nm and

20.66 nm (in diameter), respectively (Figure 4.4). The detection of nanoparticles around 20 nm with good result quality indicates that stable cross-linked polymers are obtained. The presence of a single and smooth peak suggests the absence of particle aggregation and the absence of larger particles.

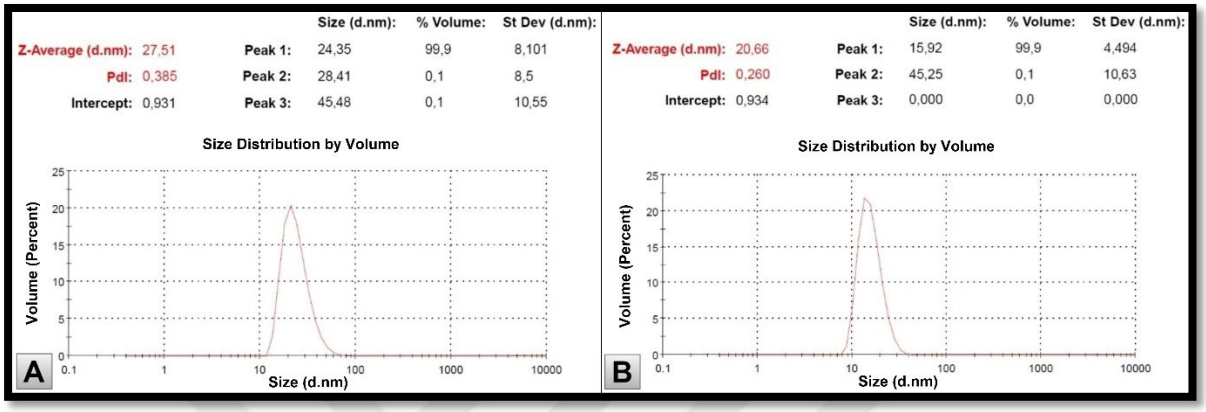

Figure 4.4. Results of dimensional analysis of **A)** Pro-MIP and **B)** NIP nanoparticles via zeta-sizer.

To analyze the surface morphology and size distributions of nanoparticles, SEM images were taken for Pro-MIP and NIP nanoparticle samples. According to the SEM images, it was observed that the sizes of Pro-MIP and NIP nanoparticles were around 20 nm, and the size distribution was homogeneous (Figure 4.5). Pro-MIP and NIP particles exhibit similar structures, and their size distributions are also comparable. Additionally, the obtained SEM results are highly consistent with the zeta-sizer measurements."

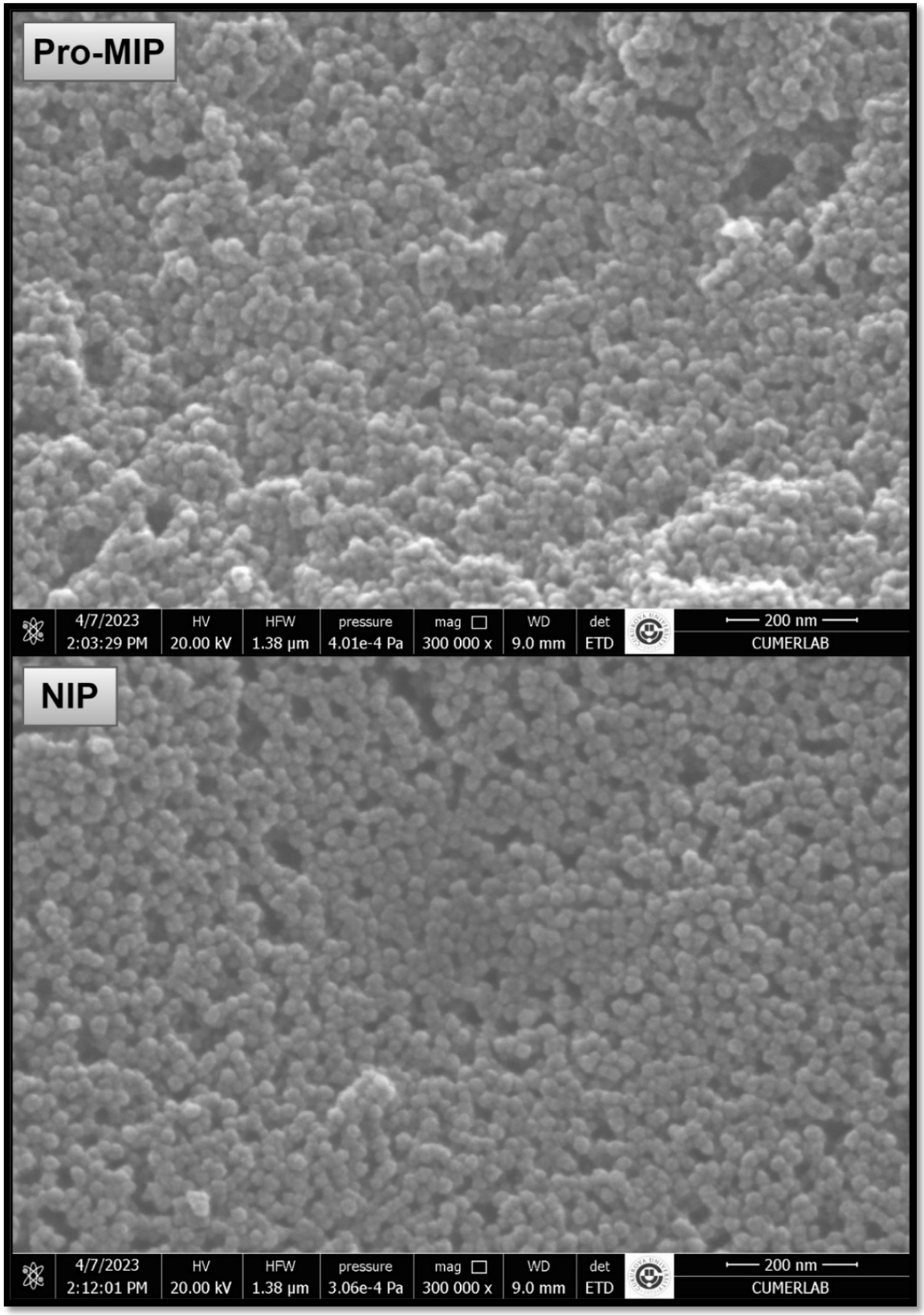

Figure 4.5. SEM images of A) Pro-MIP; and B) NIP nanoparticles.

Comparing the spectra of the L-Proline, VIM and Pro-VIM pre-complex, it can be observed that there are some similarities and differences. For example, all three samples show peaks at 3400, 3100, 1620, 1570, 1450, 1370, 1250 and 1050 cm^{-1}, which are attributed to the vibrations of the imidazole ring and the vinyl group. However, the intensities and shapes of these peaks vary depending on the degree of interaction and coordination of these groups with other functional groups. On the other hand, only L-proline and the pre-complex show peaks at 3300, 1710, 1640, 1540, 1300 and 1150 cm^{-1}, which are attributed to the vibrations of the carboxylic acid and the imino groups. These peaks indicate the presence of L-proline in the pre-complex and the formation of hydrogen bonds between the carboxylic acid and the imidazole groups. Moreover, the pre-complex shows a slightly lower peak at 1720 cm^{-1} than L-proline, which suggests that the carboxylic acid group is partially deprotonated and forms a zwitterionic structure with the imidazole group (Balachandran et al., 2014; Hasegawa et al., 2000; X.-J. Li et al., 2011; Sierra et al., 2021).

FTIR spectrum of Pro-MIP shows peaks at 1600, 1500, 1360, 1260, 1060, 870 and 760 cm^{-1}, which are attributed to the vibrations of the imidazole ring and the vinyl group. These peaks indicate the presence of the pre-complex of L-proline and VIM in the imprinted nanoparticles. On the other hand, FTIR spectrum of NIP sample does not show any of these peaks, which indicates the absence of the pre-complex or any other molecules in the non-imprinted nanoparticles. The absence of specific peaks related to L-Proline and VIM in the FTIR spectra of the non-imprinted nanoparticles is consistent with the lack of molecular imprinting and selective binding sites in these nanoparticles (Rico-Yuste & Carrasco, 2019). In conclusion, the interpretation of the FTIR spectra of the HEMA-EGDMA based L-Proline imprinted nanoparticles and non-imprinted nanoparticles can be supported by the principles of molecular imprinting, as well as the specific interactions involved in the pre-complex formation. The presence of specific peaks related to L-Proline and VIM in the FTIR spectra of the L-Proline imprinted nanoparticles, as well as their absence in the non-imprinted nanoparticles, aligns with the concepts of molecular imprinting and selective binding (El Hoshoudy et al., 2015; Rico-Yuste & Carrasco, 2019; Yahya & Abdullah, 2017; Yıldırım & Baydemir Peşint, 2021).

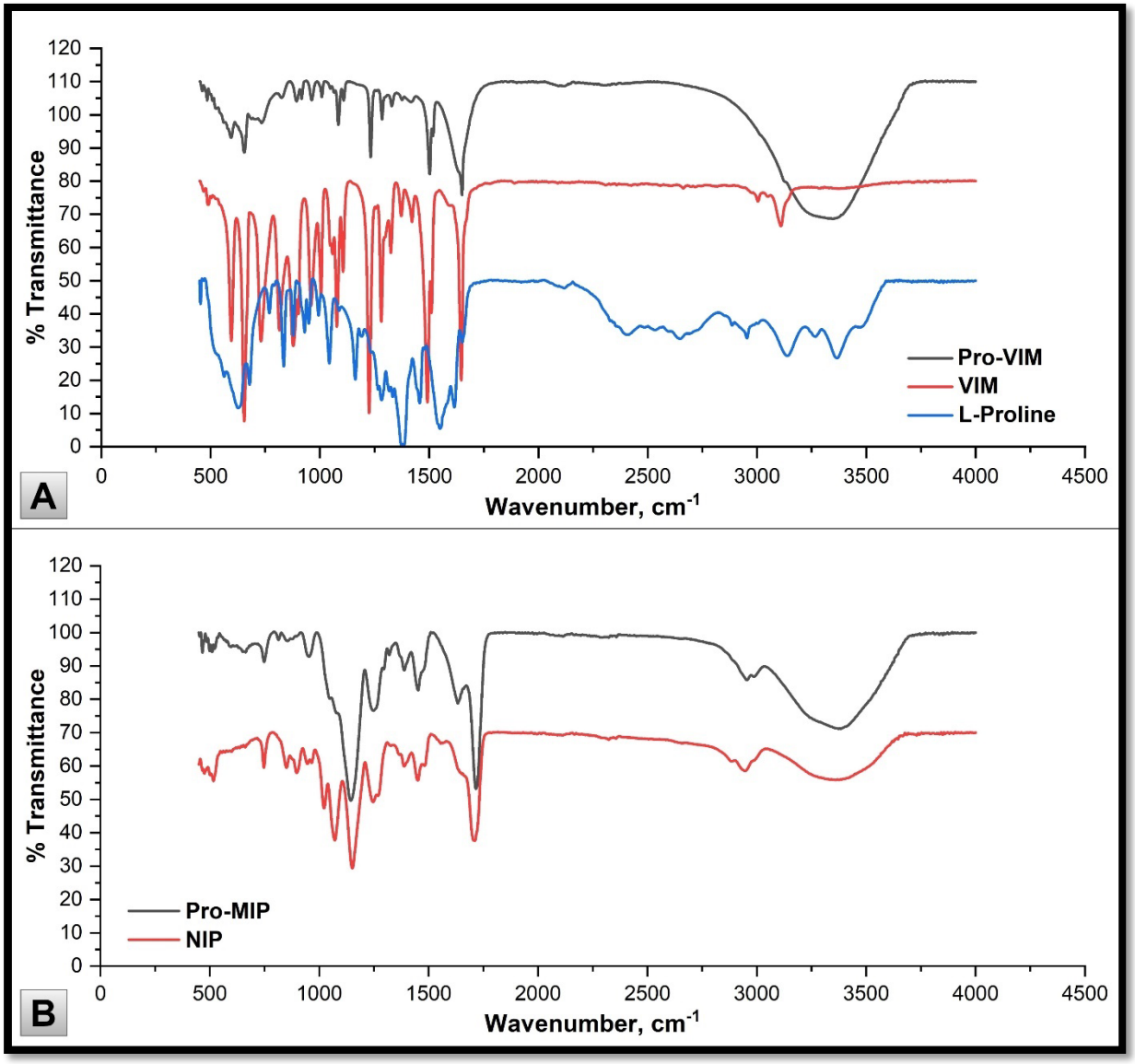

Figure 4.6. FTIR spectra of A) Pro-VIM pre-complex (1:4, n:n), VIM and L-Proline, B) Pro-MIP and NIP nanoparticles.

4.3. Template Removal Studies

To remove unreacted monomers and other components, Pro-MIP and NIP nanoparticles were washed with an ethanol/water mixture (20:80, v:v) at room temperature for 24 hours. Subsequently, Pro-MIPs were eluted by washing with an ethanol/water mixture (40:60, v:v) in batch system with a rotator to remove the L-Proline molecules. After each elution process, nanoparticles were separated via centrifugation, and the L-Proline content in the supernatant

was measured spectrophotometrically. Since the L-Proline molecule could not be measured by UV spectrophotometry without undergoing any staining process, the removal of the template molecule was monitored at 520 nm using the ninhydrin method. In this study, performing the elution cycles five times was sufficient to remove the template molecule from the structure. Despite subsequent repetitions of the process, no significant change was observed as the absorbance value approached zero. According to calculations (Equation 1 and 2), L-Proline removal rate was found to be 96%, approximately. The amount of L-Proline removed per gram of polymer was determined to be 29.52 mg.

Table 4.1. Results of template removal study.

Nanoparticle	Pro:VIM (n:n)	Amount of Pro in polymer solution (µmol)	Amount of removed Pro (µmol)	Template removal ratio (%)
Pro-MIP	1:4	0.40	0.383	96

4.4. Adsorption Studies

4.4.1. Effect of initial L-Proline concentration on adsorption

Various concentrations (0.01, 0.025, 0.05, 0.1, 0.2, 0.3, 0.45, 0.6, and 1 mg/mL) were investigated to understand the effect of initial L-Proline concentration on adsorption process. The adsorption experiments were conducted over a duration of 2 hours, allowing sufficient time for the interaction between the nanoparticles and L-Proline molecules to occur. Results showed different levels of adsorption at each concentration, reaching maximum capacities of 26.582 mg/g for Pro-MIP and 4.655 mg/g for NIP (Equation 4). These findings help us understand how initial solute concentrations influence the adsorption process and identify the best conditions for maximizing the adsorption capacities of the nanoparticles.

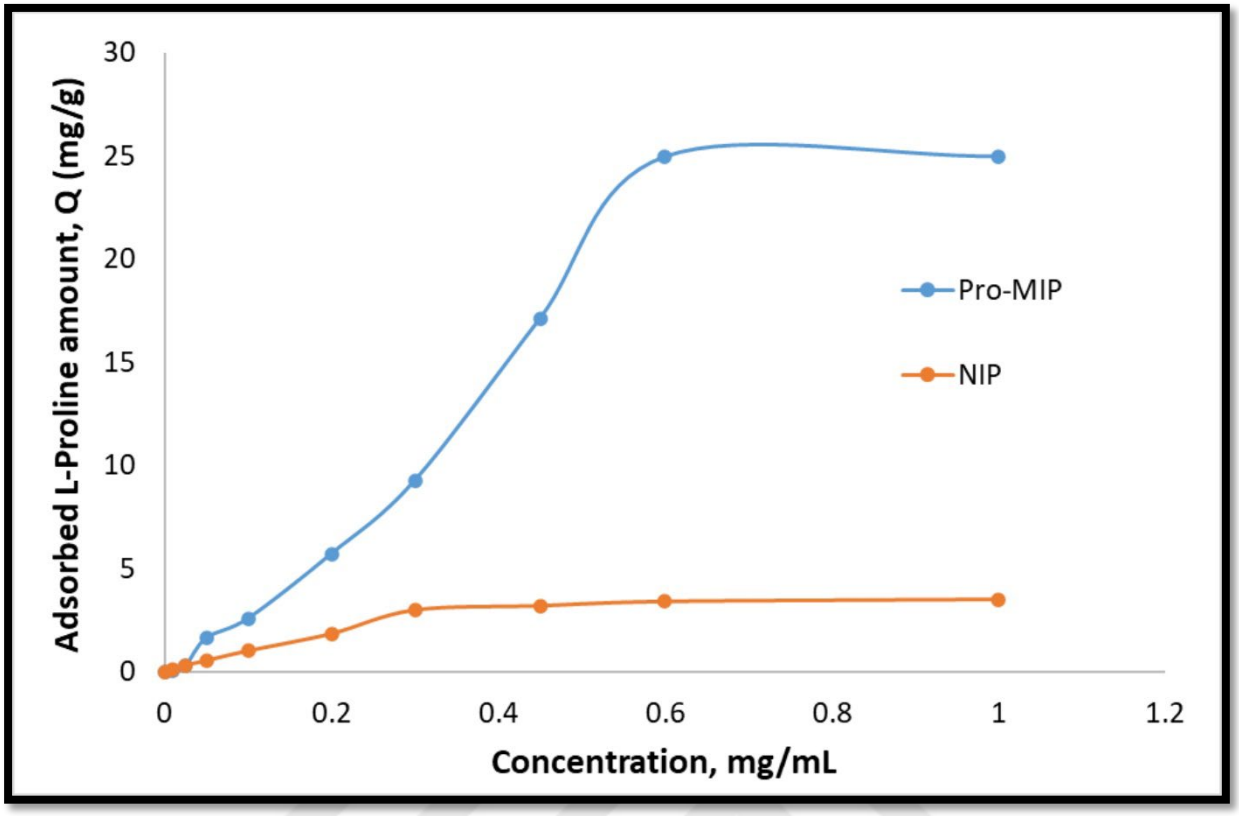

Figure 4.7. Effect of initial L-proline concentration on the maximum L-Proline adsorption (dry weight: 0.06 g, PBS pH: 7, V: 1.5 mL, 2 hours, 25°C).

The adsorption isotherms utilized in this study provide insights into the interaction between the synthesized nanoparticles and the adsorbate, L-Proline. The Langmuir Isotherm, which implies single-layer adsorption on a homogeneous surface, and the Freundlich Isotherm, which describes multi-layer adsorption on a heterogeneous surface, were employed to characterize the adsorption behavior. The Langmuir Isotherm suggests that adsorption occurs on a uniform surface, forming a monolayer of adsorbate molecules, while the Freundlich Isotherm indicates a more complex, heterogeneous surface with the formation of multiple layers.

Langmuir adsorption isotherm expressed as follows:

$$Q = Q_{max} * b * C_e / (1 + b * C_e) \quad (9)$$

Here, Q represents the actual adsorption capacity of the nanoparticles for L-Proline in mg/g, C_e denotes the equilibrium concentration of L-Proline in mg/mL, b stands for the Langmuir constant in mL/mg, and Q_{max} is the maximum L-Proline adsorption capacity in mg/g. Equation 10 can be transformed into a linear form, as shown in equation 11, and plotting $1/Q_e$ against $1/C_e$ allows the determination of $1/Q_{max}$ and $1/Q_{max}$*b from the intercept and slope, respectively.

$$C_e / Q = 1 / (Q_{max}.b) + (C_e / Q_{max}) \quad (10)$$

Freundlich adsorption isotherm can be expressed as follows:

$$Q_e = Q_f * C_e^{1/n} \quad (11)$$

In this equation, Q_e represents the amount of L-Proline adsorption in mg/g, while C_e stands for the equilibrium L-Proline concentration in the solution in mg/mL. Q_f represents the maximum Freundlich adsorption capacity in mg/g, and 1/n signifies Freundlich constants indicating the intensity of adsorption. To linearize this equation, logarithms were taken on both sides, resulting in a linear form. The natural logarithm of C_e ($\ln C_e$) was plotted against the natural logarithm of Q_e ($\ln Q_e$) to determine the values of 1/n and Q_f from the intercept and slope.

$$\ln Q_e = \ln Q_f + (1/n * \ln C_e) \quad (12)$$

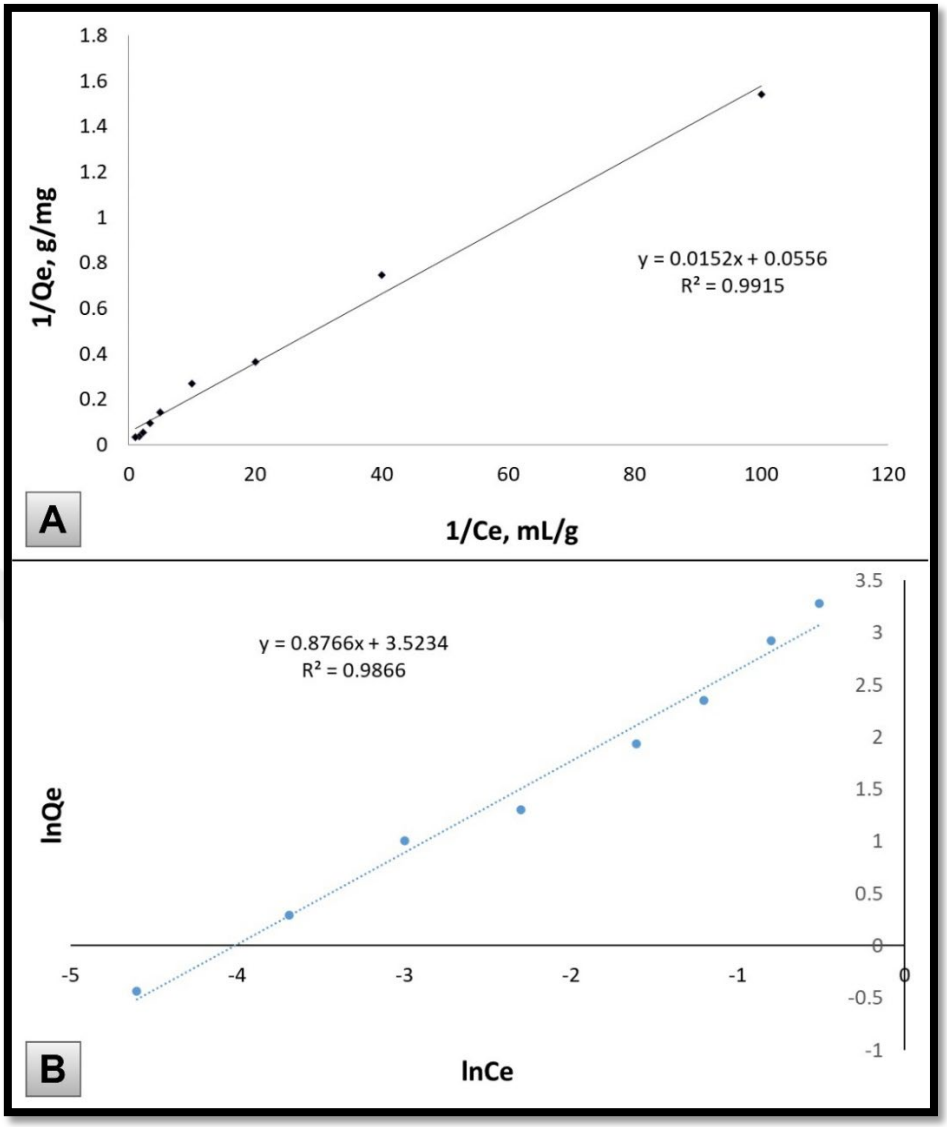

Figure 4.8. Adsorption isotherms. The plot of A) Langmuir and B) Freundlich isotherms.

Table 4.2. Adsorption isotherms (w_{dry}: 0.06 g, PBS pH: 7, V: 1.5 mL, 2 hours, 25°C).

Experimental	**Langmuir Constants**			**Freundlich Constants**		
Q_{ex}	Q_L	b	R^2	Q_F	n	R^2
(mg/g)	(mg/g)	(mL/mg)		(mg/g)		
26.5	19.8	3.6	0.99	33.9	1.14	0.98

The Langmuir isotherm yielded a higher correlation coefficient (R2) of 0.9915 compared to the Freundlich isotherm (0.9866). The calculated maximum adsorption amount (Qmax) using the Langmuir model was 19.8 mg/g, aligning more closely with the experimentally obtained data (26.5 mg/g) than the Freundlich model (33.9 mg/g). The Freundlich adsorption isotherm constant (n) was determined to be 1.14, and the Langmuir constant (b) was obtained as 3.6. Based on calculations, it was observed that the experimental data exhibited better alignment with the Langmuir adsorption isotherm, indicating that the adsorption process is more consistent with single-layer adsorption on a homogeneous surface.

4.4.2. Effect of temperature on adsorption

The investigation focused on understanding the impact of temperature on the adsorption process, examining four distinct temperatures: 4°C, 25°C, 37°C, and 45°C. Following a 2-hour adsorption period in batch system in a rotator, notable results were obtained. Particularly, the maximum L-Proline adsorption capacity was identified at 25°C, with Pro-MIP reaching a value of 26.582 mg/g. It was observed that L-Proline adsorption significantly decreased at higher (20.699 mg/g at 4°C) and lower temperatures (18.987 mg/g at 45°C). This finding underscores that 25°C stands out as the temperature yielding the most favorable adsorption of L-Proline molecule onto Pro-MIP, emphasizing the crucial role of temperature in influencing the adsorption characteristics.

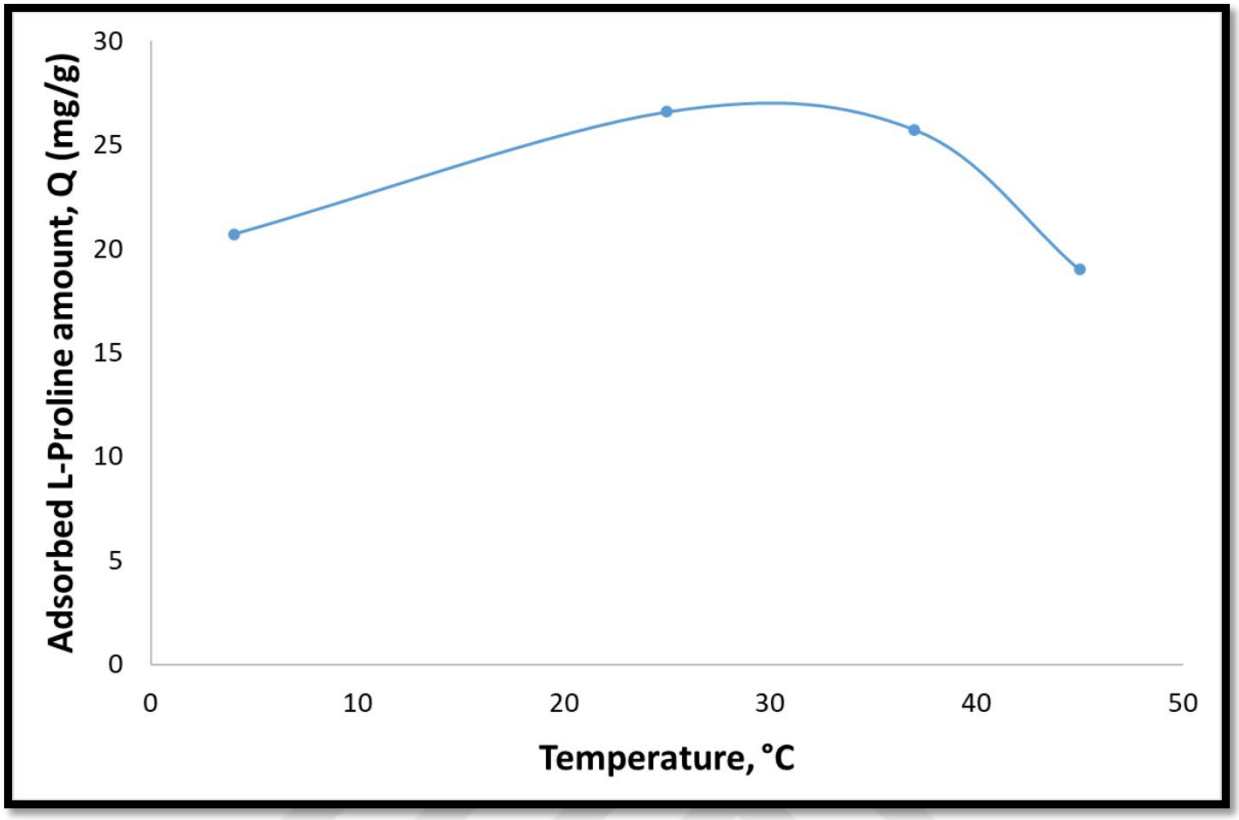

Figure 4.9. Effect of temperature on maximum L-proline adsorption (dry weight: 0.06 g, concentration: 0.6 mg/mL, PBS pH: 7, V: 1.5 mL, 2 hours).

4.4.3. Effect of interaction time on adsorption

To understand the influence of interaction time on adsorption, 0.36 mg of nanoparticles was taken into a falcon tube, and adsorption experiments were conducted in a batch system at 25°C using a rotator. Samples (1.5 mL) were collected at specific time intervals (0, 5, 15, 30, 45, 60, 90, 120 minutes), followed by centrifugation at 18,000 rpm. The supernatant was then subjected to spectrophotometric analysis using ninhydrin reagent. The supernatant from each sample was then measured spectrophotometrically using a ninhydrin reagent. The results of the study showed that the adsorption process stabilizes after 90 minutes. Furthermore, the optimal adsorption time, which is the time required for maximum adsorption, was determined to be 2 hours.

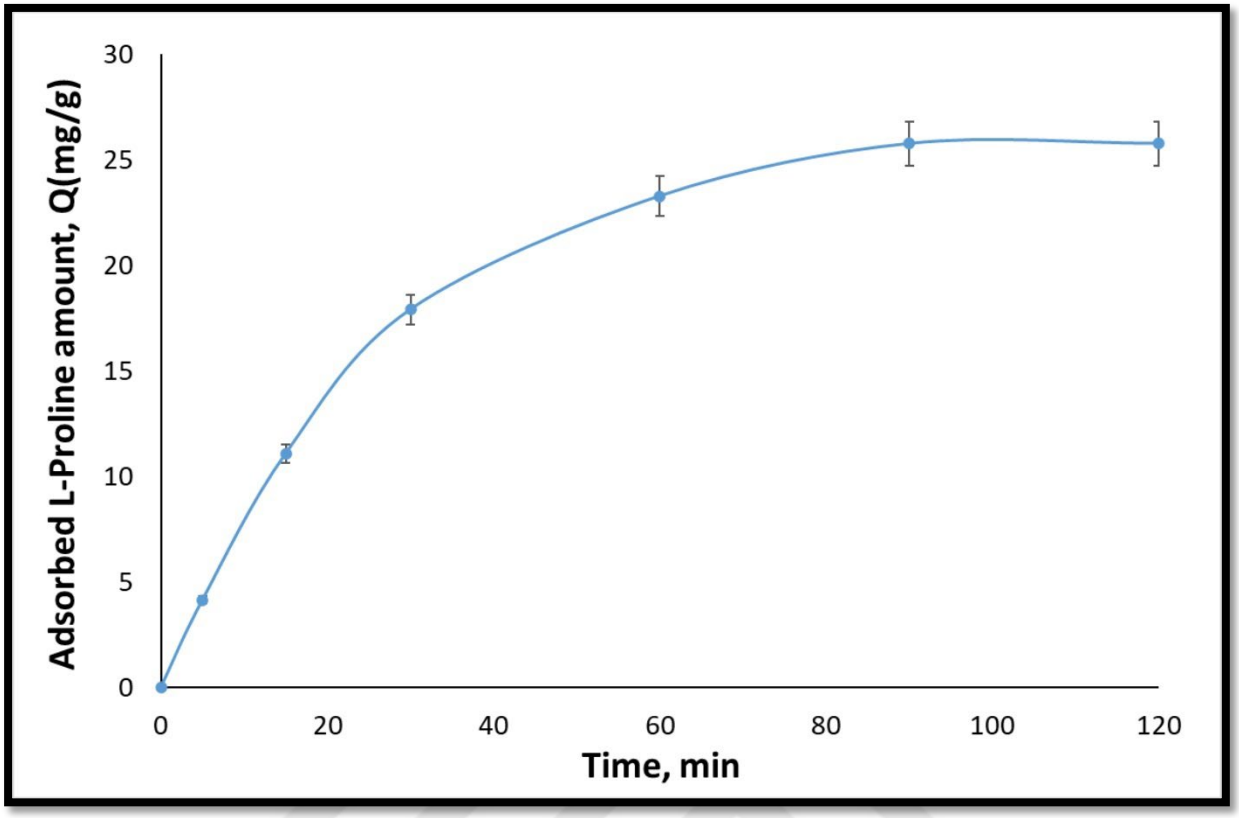

Figure 4.10. Effect of interaction time on maximum L-proline adsorption (dry weight: 0.36 g, concentration: 0.6 mg/mL, PBS pH: 7, V: 9 mL, 25 °C).

Adsorption kinetics provides insight into the process of molecules sticking to a surface by examining the quantity of attached molecules at the solid-solution interface. The mechanisms governing the adsorption process, such as mass transfer and diffusion-controlled chemical reactions, can be assessed through the application of kinetic models. In this study, the data on the amount of adsorption over time were subjected to both first- and second-order kinetic models to identify the controlling mechanisms of the adsorption process. This analytical approach allows for the determination of the key factors influencing the adsorption kinetics. The utilization of such kinetic models enhances our ability to comprehend and predict the behavior of adsorption systems, contributing to a more comprehensive understanding of the adsorption phenomena.

Lagergren's first-order rate equation, whose equation is given below, is used.

$$\Delta Qt/dt = k1*(Qe-Qt) \quad (13)$$

In here, k1 is first order adsorption rate constant (1/min); Qe and Qt are L-Proline adsorption amount at equilibrium and at time t (mg/g), respectively. This equation was linearized as equation 14 and plotted log(Qe-Qt) versus t to obtain Qe and k1 from the cut-off point and slope.

$$\log(Qe-Qt) = \log(Qe) – (k1*t)/2.303 \quad (14)$$

The pseudo-second-order equation expressed as:

$$\Delta Qt /dt = k2*(Qe-Qt)2 \quad (15)$$

k2 is pseudo-second-order adsorption rate constant (g/mg.min).

It was linearized as equation 16 and plotted (t/Qt) versus “t” to obtain “Qe” and “k2” from the cut-off point and slope;

$$(t/Qt) = (1/k2*Qe\ 2\ ) + (1/Qe)*\ t \quad (16)$$

Figures 4.12 present the plots for pseudo-first and pseudo-second-order kinetics. The rate constants and the amounts of adsorbed L-Proline at both experimental and equilibrium times are detailed in Table 4.4. Analysis of the data reveals that the correlation coefficients for pseudo-second-order kinetics surpass those for pseudo-first-order kinetics. Moreover, the proximity of the experimental Qe values to those derived from pseudo-second-order kinetics suggests that the adsorption aligns better with pseudo-second-order kinetics. This observation implies that the chemically controlled adsorption of L-Proline molecules onto Pro-MIP nanoparticles governs the rate-determining step in the adsorption process, shedding light on the underlying dynamics.

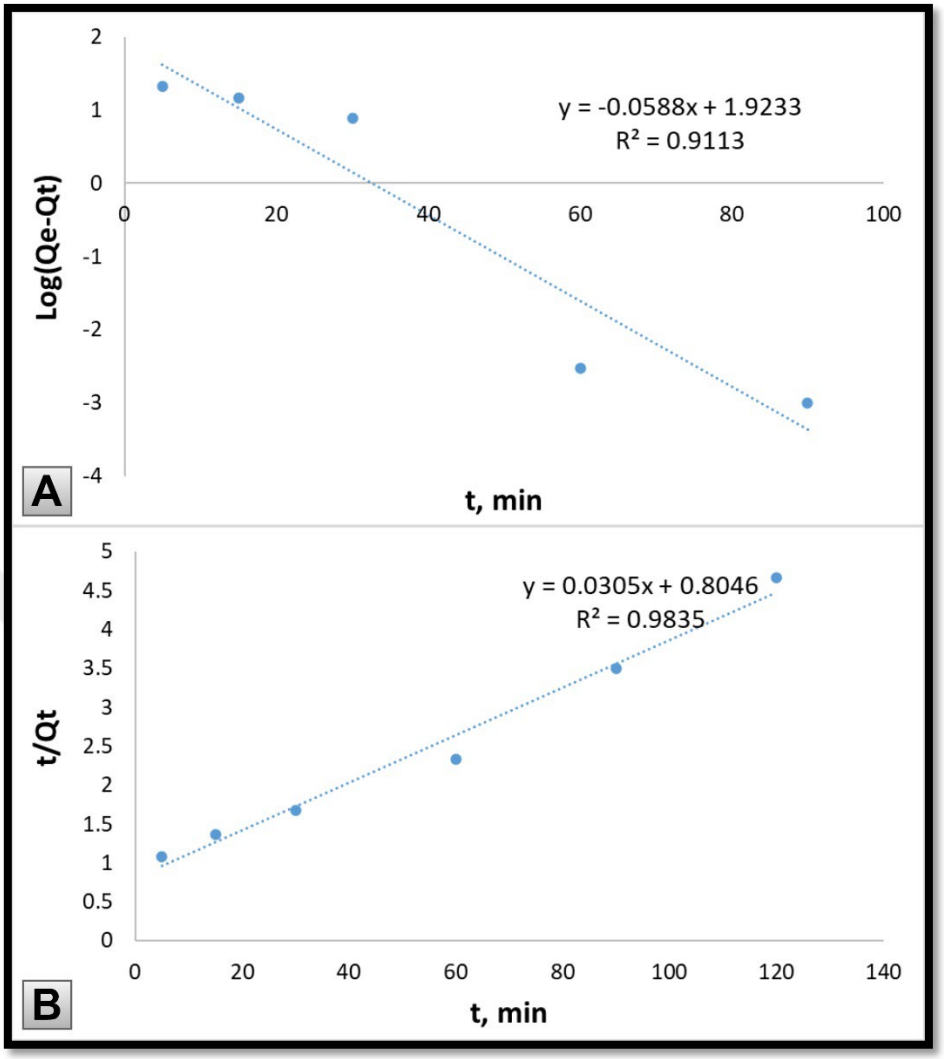

Figure 4.11. The plot of **A)** pseudo first order kinetics and **B)** pseudo second order kinetics.

Table 4.3. Adsorption kinetics model constants and adsorption amounts.

Initial Concentration (mg/mL)	**Experimental**	**Pseudo-first-order-kinetic**			**Pseudo-second-order-kinetic**		
	Q_{eq} (mg/g)	k1 (1/dk)	Q_{eq} (pg/g)	R^2	k2 (1/dk)	Q_{eq} (pg/g)	R^2
0.60	26.5	0.135	6.84	0.9113	0.0007484	32.78	0.9835

4.5. Selectivity Studies

According to the LC-MS/MS chromatograms, it is observed that the initial amount of L-proline significantly decreases after adsorption. The high desorption amount also demonstrates the strong adsorption of L-proline molecules to the nanoparticles. The relatively close values before and after adsorption for competitor molecules, along with the notably low desorption, indicate the high selectivity of Pro-MIP nanoparticles for L-proline in presence of competitors. In figure 14D, the seperation of L-Proline from human serum spiked with all the competitor molecules, was successfully confirmed. The imprinting factor provided in Table 5 reveal that Pro-MIP nanoparticles adsorb L-proline more effectively than NIP nanoparticles. In addition, selectivity coefficient values show that Pro-MIP nanoparticles can adsorb L-proline approximately 4 times better than L-Histidine and around 17.2 times better than L-Phenylalanine.

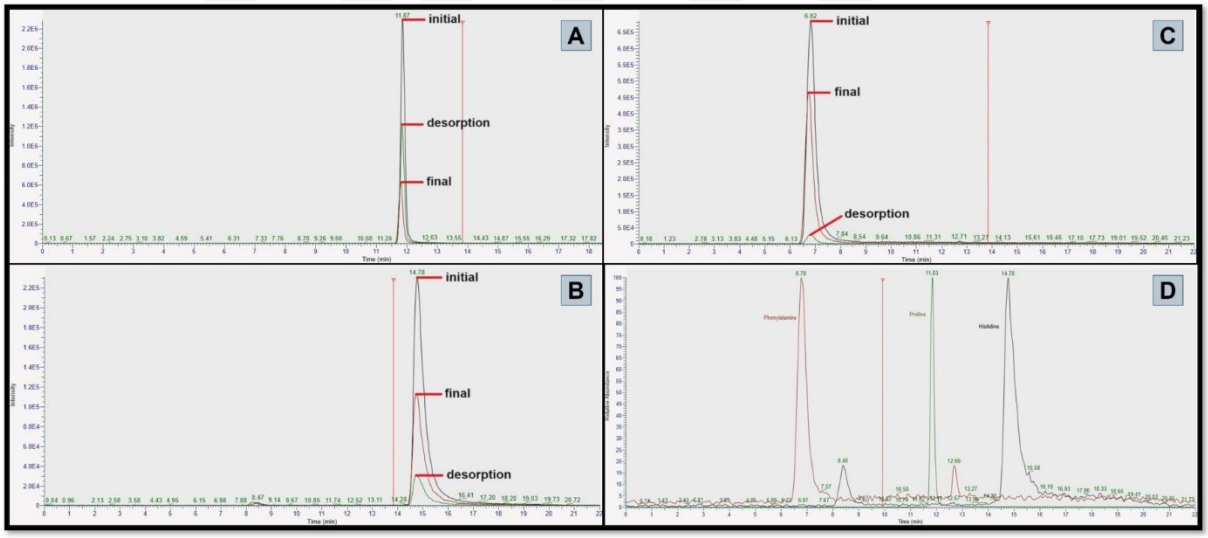

Figure 4.12. LC-MS/MS analysis results of A) L-Proline, B) L-Histidine, C) L-Phenylalanine, and D) human serum spiked with complex medium (L-Proline + L-Histidine + L-Phenylalanine).

Table 4.4. Selectivity study. Comparison of binding amounts, imprinting factors and selectivity coefficients.

Competitors	Pro-MIP	NIP		
	Q (mg/g)	Q (mg/g)	IF	k
L-Proline	25	8	3.09	
L-Histidine	6.25	5.1	1.2	4
L-Phenylalanine	1.45	0.97	1.49	17.2

4.6. Desorption and Reusability Studies

Ensuring that biomaterials can be used repeatedly is of great importance. The adsorption and desorption processes of L-Proline aqueous solution onto and from Pro-MIP were repeated for 10 cycles. After 10 cycles, nanoparticles maintained 94.394% of their initial adsorption capacity.

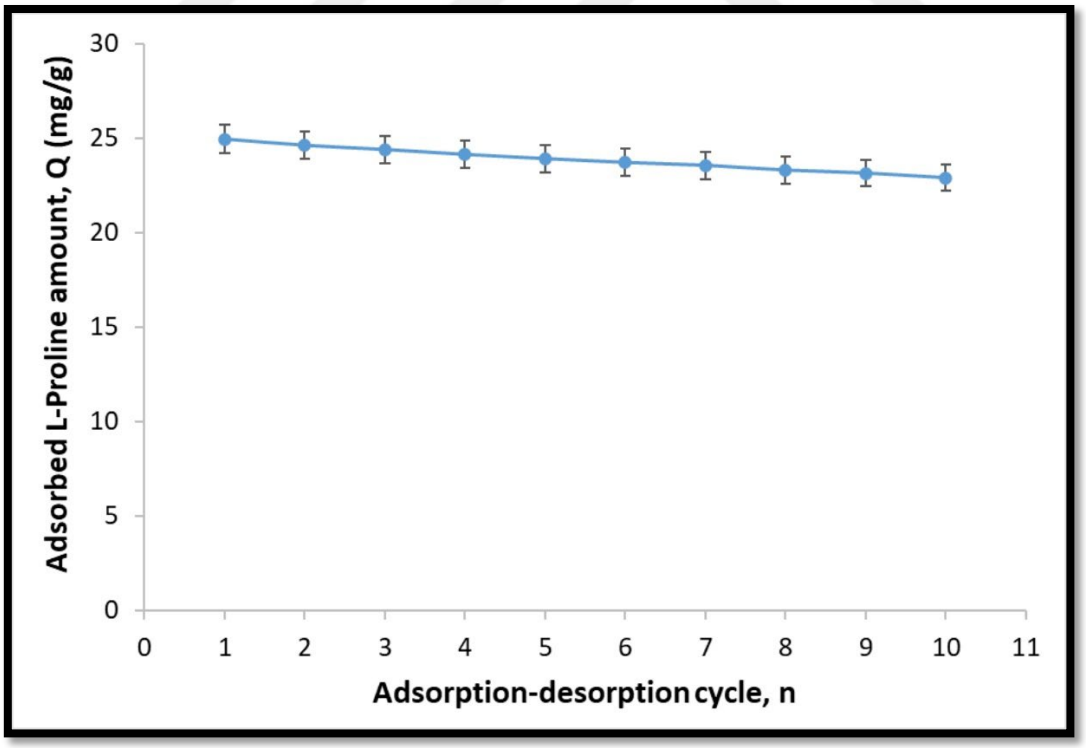

Figure 4.13. Reusability studies under optimized conditions.

5. CONCLUSION

In the context of this thesis study, molecularly imprinted nanoparticles were synthesized with the primary goal of selectively recognizing the L-Proline molecule from human serum. The synthesis of HEMA-based nanoparticles was carried out through emulsion polymerization, and synthesized nanoparticles were characterized using scanning electron microscopy (SEM) analysis and size determination techniques. The polymerization process exhibited a commendable yield with Pro-MIP achieving 93.22%, while NIP demonstrated a higher yield at 98.36%. Zeta-sizer analysis was used in estimating the diameters of Pro-MIP and NIP nanoparticles, revealing approximate dimensions of 27.51 nm and 20.66 nm, respectively. These findings were further confirmed through SEM analysis, affirming the accuracy of the size measurements. In the realm of adsorption studies, Pro-MIP nanoparticles demonstrated a notable maximum L-Proline adsorption capacity of 26.58 mg/g, surpassing NIP, which exhibited a capacity of 4.65 mg/g. This difference in adsorption capacities underscores the effective imprinting of L-Proline within the molecular structure of Pro-MIPs. The selectivity of L-Proline imprinted nanoparticles was successfully validated through LC-MS/MS, even in the presence of competing molecules such as L-Histidine and L-Phenylalanine, and in the complex matrix of human serum. This robust selectivity substantiates the potential applicability of Pro-MIPs in complex biological environments. Furthermore, the practical utility of Pro-MIPs was demonstrated through repeated adsorption-desorption cycles, highlighting their notable reusability for up to 10 cycles without a significant decline in selective adsorption capacity. This attribute enhances the economic feasibility and sustainable application of L-Proline imprinted nanoparticles in various fields, ranging from analytical chemistry to biomedicine.

KAYNAKÇA

Abdalla, A. M., Elnaghi, B. E., Hossain, S., Dawood, M., Abdelrehim, O., & Azad, A. K. (2020). Nanotechnology utilization in energy conversion, storage and efficiency: A perspective review. *Advanced Energy Conversion Materials*, *1*(1), 30–54.

Ábrahám, E., Hourton-Cabassa, C., Erdei, L., & Szabados, L. (2010). Methods for determination of proline in plants. *Plant Stress Tolerance: Methods and Protocols*, 317–331.

Adzhubei, A. A., Sternberg, M. J. E., & Makarov, A. A. (2013). Polyproline-II helix in proteins: structure and function. *Journal of Molecular Biology*, *425*(12), 2100–2132.

Albaugh, V. L., Mukherjee, K., & Barbul, A. (2017). Proline precursors and collagen synthesis: biochemical challenges of nutrient supplementation and wound healing. *The Journal of Nutrition*, *147*(11), 2011–2017.

Alexander, C., Andersson, H. S., Andersson, L. I., Ansell, R. J., Kirsch, N., Nicholls, I. A., O'Mahony, J., & Whitcombe, M. J. (2006). Molecular imprinting science and technology: A survey of the literature for the years up to and including 2003. *Journal of Molecular Recognition*, *19*(2), 106–180. https://doi.org/10.1002/jmr.760

Allen, W. D., Czinki, E., & Császár, A. G. (2004). Molecular structure of proline. *Chemistry–A European Journal*, *10*(18), 4512–4517.

Alvarez, M. E., Savouré, A., & Szabados, L. (2022). Proline metabolism as regulatory hub. *Trends in Plant Science*, *27*(1), 39–55.

Ameen, F., Alsamhary, K., Alabdullatif, J. A., & ALNadhari, S. (2021). A review on metal-based nanoparticles and their toxicity to beneficial soil bacteria and fungi. *Ecotoxicology and Environmental Safety*, *213*, 112027.

Andaç, M., Baydemir, G., Yavuz, H., & Denizli, A. (2012). Molecularly imprinted composite cryogel for albumin depletion from human serum. *Journal of Molecular Recognition*, *25*(11), 555–563. https://doi.org/10.1002/jmr.2202

Andaç, M., Galaev, I. Y., & Denizli, A. (2016). Affinity based and molecularly imprinted cryogels: Applications in biomacromolecule purification. *Journal of Chromatography B*, *1021*, 69–80.

Andersson, L. I. (2000). Molecular imprinting: developments and applications in the analytical chemistry field. *Journal of Chromatography B: Biomedical Sciences and Applications*, *745*(1), 3–13.

Arshady, R., & Mosbach, K. (1981). Synthesis of substrate-selective polymers by host-guest polymerization. *Die Makromolekulare Chemie: Macromolecular Chemistry and Physics*, *182*(2), 687–692.

Aylaz, G., Zenger, O., Baydemir Peşint, G., & Andaç, M. (2022). Molecularly imprinted composite discs for transferrin recognition. *Separation Science and Technology*, *57*(9), 1359–1375.

Balachandran, V., Boobalan, M., Amaladasan, M., & Velmathi, S. (2014). Synthesis and Vibrational Spectroscopic Investigation of Methyl L-Prolinate Hydrochloride: A Computational Insight. *Spectroscopy Letters*, *47*(9), 676–689.

Bayda, S., Adeel, M., Tuccinardi, T., Cordani, M., & Rizzolio, F. (2019). The history of nanoscience and nanotechnology: from chemical–physical applications to nanomedicine. *Molecules*, *25*(1), 112.

Behzad, F., Naghib, S. M., Tabatabaei, S. N., Zare, Y., & Rhee, K. Y. (2021). An overview of the plant-mediated green synthesis of noble metal nanoparticles for antibacterial applications. *Journal of Industrial and Engineering Chemistry*, *94*, 92–104.

Beighton, P. (1970). Ehlers-Danlos syndrome. *Annals of the Rheumatic Diseases*, *29*(3), 332.

Bennick, A. (1982). Salivary proline-rich proteins. *Molecular and Cellular Biochemistry*, *45*, 83–99.

Bennick, A. (1987). Structural and genetic aspects of proline-rich proteins. *Journal of Dental Research*, *66*(2), 457–461.

Bergmann, N. M., & Peppas, N. A. (2008). Molecularly imprinted polymers with specific recognition for macromolecules and proteins. *Progress in Polymer Science*, *33*(3), 271–288.

Bojarska, J., Kaczmarek, K., Zabrocki, J., & Wolf, W. M. (2019). Amino acids: molecules of life. *Int. J. Nutr. Sci*, *4*, 1035–1037.

Bröer, S. (2022). Amino acid transporters as modulators of glucose homeostasis. *Trends in Endocrinology & Metabolism*, *33*(2), 120–135.

Casado, C., Castan, J., Gracia, I., Yus, M., Mayoral, A., Sebastian, V., López-Ram-de-Viu, P., Uriel, S., & Coronas, J. (2012). L-and D-proline adsorption by chiral ordered mesoporous silica. *Langmuir*, *28*(16), 6638–6644.

Chang, P., Zhang, Z., & Yang, C. (2010). Molecularly imprinted polymer-based chemiluminescence array sensor for the detection of proline. *Analytica Chimica Acta*, *666*(1–2), 70–75.

Chen, L., Xu, S., & Li, J. (2011). Recent advances in molecular imprinting technology: Current status, challenges and highlighted applications. *Chemical Society Reviews*, *40*(5), 2922–2942. https://doi.org/10.1039/c0cs00084a

Chen, S., White, C. E., diCenzo, G. C., Zhang, Y., Stogios, P. J., Savchenko, A., & Finan, T. M. (2016). L-Hydroxyproline and D-proline catabolism in Sinorhizobium meliloti. *Journal of Bacteriology*, *198*(7), 1171–1181.

Clark, W. T., & Radivojac, P. (2011). Analysis of protein function and its prediction from amino acid sequence. *Proteins: Structure, Function, and Bioinformatics*, *79*(7), 2086–2096.

COSKUN, M. G., COPUR, O. U., & OMEROGLU, P. Y. (2017). Application of Nanotechnology in Food Packaging. *Eurasian Journal of Food Science and Technology*, *1*(2), 59–66.

Dainiak, M. B., Galaev, I. Y., Kumar, A., Plieva, F. M., & Mattiasson, B. (2007). Chromatography of living cells using supermacroporous hydrogels, cryogels. In *Advances in Biochemical Engineering/Biotechnology* (Vol. 106, pp. 101–127). Springer Berlin Heidelberg. https://doi.org/10.1007/10_2006_044

Deschepper, K., & DeGroote, G. (1995). Effect of dietary protein, essential and non-essential amino acids on the performance and carcase composition of male broiler chickens. *British Poultry Science*, *36*(2), 229–245.

Dhand, C., Dwivedi, N., Loh, X. J., Ying, A. N. J., Verma, N. K., Beuerman, R. W., Lakshminarayanan, R., & Ramakrishna, S. (2015). Methods and strategies for the synthesis of diverse nanoparticles and their applications: a comprehensive overview. *Rsc Advances*, *5*(127), 105003–105037.

Donohue, J., & Trueblood, K. (1952). The crystal structure of hydroxy-L-proline. II. Determination and description of the structure. *Acta Crystallographica*, *5*(4), 419–431.

Drexler, K. E. (2004). Nanotechnology: from Feynman to funding. *Bulletin of Science, Technology & Society*, *24*(1), 21–27.

El Hoshoudy, A., Desouky, S., Al-sabagh, A., El-kady, M., Betiha, M., & Mahmoud, S. (2015). Synthesis and characterization of polyacrylamide crosslinked copolymer for enhanced oil recovery and rock wettability alteration. *International Journal of Oil, Gas and Coal Engineering*, *3*(4), 43–55.

Ertürk, G., & Mattiasson, B. (2017). Molecular imprinting techniques used for the preparation of biosensors. *Sensors*, *17*(2), 288.

Forlani, G., & Funck, D. (2020). A specific and sensitive enzymatic assay for the quantitation of L-proline. *Frontiers in Plant Science*, *11*, 582026.

Gałęzowska, G., Ratajczyk, J., & Wolska, L. (2021). Determination of amino acids in human biological fluids by high-performance liquid chromatography: Critical review. *Amino Acids*, *53*(7), 993–1009.

Green, N. M., & Lowther, D. A. (1959). Formation of collagen hydroxyproline in vitro. *Biochemical Journal*, *71*(1), 55.

Hansen, D. E. (2007). Recent developments in the molecular imprinting of proteins. *Biomaterials*, *28*(29), 4178–4191.

Hasanzadeh, M, Baghban, H. N., & Shadjou, N. (2018). Non-enzymatic determination of L-Proline amino acid in unprocessed human plasma sample using hybrid of graphene quantum dots decorated with gold nanoparticles and poly cysteine: a novel signal amplification strategy. *Analytical Sciences*, *34*(3), 355–362.

Hasanzadeh, Mohammad, Nahar, A. S., Hassanpour, S., Shadjou, N., Mokhtarzadeh, A., & Mohammadi, J. (2017). Proline dehydrogenase-entrapped mesoporous magnetic silica nanomaterial for electrochemical biosensing of L-proline in biological fluids. *Enzyme and Microbial Technology*, *105*, 64–76.

Hasegawa, K., Ono, T., & Noguchi, T. (2000). Vibrational spectra and ab initio DFT calculations of 4-methylimidazole and its different protonation forms: infrared and Raman markers of the protonation state of a histidine side chain. *The Journal of Physical Chemistry B*, *104*(17), 4253–4265.

Hayat, S., Hayat, Q., Alyemeni, M. N., Wani, A. S., Pichtel, J., & Ahmad, A. (2012). Role of proline under changing environments: a review. *Plant Signaling & Behavior*, *7*(11), 1456–1466.

Heger, J. (2003). Essential to non-essential amino acid ratios. In *Amino acids in animal nutrition* (pp. 103–124). CABI publishing Wallingford UK.

Hill, J. W., & Nemoto, E. M. (2016). N-acetyl proline-glycine-proline: implications for neurological disorders. *Neural Regeneration Research*, *11*(6), 898.

Hu, C. A., Phang, J. M., & Valle, D. (2008). Proline metabolism in health and disease. *Amino Acids*, *35*, 651–652.

Hulkoti, N. I., & Taranath, T. C. (2014). Biosynthesis of nanoparticles using microbes—a review. *Colloids and Surfaces B: Biointerfaces*, *121*, 474–483.

Jacquet, H., Demily, C., Houy, E., Hecketsweiler, B., Bou, J., Raux, G., Lerond, J., Allio, G., Haouzir, S., & Tillaux, A. (2005). Hyperprolinemia is a risk factor for schizoaffective disorder. *Molecular Psychiatry*, *10*(5), 479–485.

Johnson, J. C., & Korley, L. T. J. (2012). Enhanced mechanical pathways through nature's building blocks: amino acids. *Soft Matter*, *8*(45), 11431–11442.

Kampel, D., Kupferschmidt, R., & Lubec, G. (1990). Toxicity of D-proline. *Amino Acids: Chemistry, Biology and Medicine*, 1164–1171.

Karna, E., Szoka, L., Huynh, T. Y. L., & Palka, J. A. (2020). Proline-dependent regulation of collagen metabolism. *Cellular and Molecular Life Sciences*, *77*, 1911–1918.

Kay, B. K., Williamson, M. P., & Sudol, M. (2000). The importance of being proline: the interaction of proline-rich motifs in signaling proteins with their cognate domains. *The FASEB Journal*, *14*(2), 231–241.

Khan, Y., Sadia, H., Ali Shah, S. Z., Khan, M. N., Shah, A. A., Ullah, N., Ullah, M. F., Bibi, H., Bafakeeh, O. T., & Khedher, N. Ben. (2022). Classification, synthetic, and characterization approaches to nanoparticles, and their applications in various fields of nanotechnology: A review. *Catalysts*, *12*(11), 1386.

Kijowska-Oberc, J., Staszak, A. M., Wawrzyniak, M. K., & Ratajczak, E. (2020). Changes in proline levels during seed development of orthodox and recalcitrant seeds of genus Acer in a climate change scenario. *Forests*, *11*(12), 1362.

Kitadai, N., & Maruyama, S. (2018). Origins of building blocks of life: A review. *Geoscience Frontiers*, *9*(4), 1117–1153.

Kolahalam, L. A., Viswanath, I. V. K., Diwakar, B. S., Govindh, B., Reddy, V., & Murthy, Y. L. N. (2019). Review on nanomaterials: Synthesis and applications. *Materials Today: Proceedings*, *18*, 2182–2190.

Kosiol, C., Goldman, N., & Buttimore, N. H. (2004). A new criterion and method for amino acid classification. *Journal of Theoretical Biology*, *228*(1), 97–106.

Kushwaha, A., Goswami, L., & Kim, B. S. (2022). Nanomaterial-based therapy for wound healing. *Nanomaterials*, *12*(4), 618.

Liang, S., Sanchez-Espiridion, B., Xie, H., Ma, J., Wu, X., & Liang, D. (2015). Determination of proline in human serum by a robust LC-MS/MS method: application to identification of human metabolites as candidate biomarkers for esophageal cancer early detection and risk stratification. *Biomedical Chromatography*, *29*(4), 570–577.

Liang, X., Zhang, L., Natarajan, S. K., & Becker, D. F. (2013). Proline mechanisms of stress survival. *Antioxidants & Redox Signaling*, *19*(9), 998–1011.

Li, D., Guan, T., He, Y., Liu, F., Yang, A., He, Q., Shen, Z., & Xin, M. (2018). A chiral sensor based on weak measurement for the determination of Proline enantiomers in diverse measuring circumstances. *Biosensors and Bioelectronics*, *110*, 103–109.

Li, P., & Wu, G. (2018). Roles of dietary glycine, proline, and hydroxyproline in collagen synthesis and animal growth. *Amino Acids*, *50*, 29–38.

Li, P., Yin, Y.-L., Li, D., Kim, S. W., & Wu, G. (2007). Amino acids and immune function. *British Journal of Nutrition*, *98*(2), 237–252.

Li, X.-J., Zhong, Z.-J., & Wu, H.-Z. (2011). DFT and MP2 investigations of L-proline and its hydrated complexes. *Journal of Molecular Modeling*, *17*, 2623–2630.

Mahoney, N. M., Janmey, P. A., & Almo, S. C. (1997). Structure of the profilin-poly-L-proline complex involved in morphogenesis and cytoskeletal regulation. *Nature Structural Biology*, *4*(11), 953–960.

Maity, T., Paul, S., & De, P. (2023). Side-chain amino acid-based macromolecular architectures. *Journal of Macromolecular Science, Part A*, *60*(1), 2–17.

Malik, S., Muhammad, K., & Waheed, Y. (2023). Nanotechnology: A revolution in modern industry. *Molecules*, *28*(2), 661.

Martín-Esteban, A. (2013). Molecularly-imprinted polymers as a versatile, highly selective tool in sample preparation. *TrAC Trends in Analytical Chemistry*, *45*, 169–181.

Mauter, M. S., Zucker, I., Perreault, F., Werber, J. R., Kim, J.-H., & Elimelech, M. (2018). The role of nanotechnology in tackling global water challenges. *Nature Sustainability*, *1*(4), 166–175.

Maynard, A. D. (2007). Nanotechnology: the next big thing, or much ado about nothing? *The Annals of Occupational Hygiene*, *51*(1), 1–12.

Merdas, S. M. (2021). Molecular Imprinting: Fundamentals and Applications. *University of Thi-Qar Journal*, *16*(2), 19–51.

Mertz, E. T., Beeson, W. M., & Jackson, H. D. (1952). Classification of essential amino acids for the weanling pig. *Archives of Biochemistry and Biophysics*, *38*(1), 121–128.

Mitran, V., Albu, M. G., Vasile, E., Cimpean, A., & Costache, M. (2015). Dose-related effects of sericin on preadipocyte behavior within collagen/sericin hybrid scaffolds. *Progress in Natural Science: Materials International*, *25*(2), 122–130.

Mitsubuchi, H., Nakamura, K., Matsumoto, S., & Endo, F. (2008). Inborn errors of proline metabolism. *The Journal of Nutrition*, *138*(10), 2016S-2020S.

Mitsubuchi, H., Nakamura, K., Matsumoto, S., & Endo, F. (2014). Biochemical and clinical features of hereditary hyperprolinemia. *Pediatrics International*, *56*(4), 492–496.

Mjalli, F. S. (2016). Novel amino acids based ionic liquids analogues: Acidic and basic amino acids. *Journal of the Taiwan Institute of Chemical Engineers*, *61*, 64–74.

Morgan, A. A., & Rubenstein, E. (2013). Proline: the distribution, frequency, positioning, and common functional roles of proline and polyproline sequences in the human proteome. *PloS One*, *8*(1), e53785.

Nagamune, T. (2017). Biomolecular engineering for nanobio/bionanotechnology. *Nano Convergence*, *4*(1), 9.

Namavar, Y., Duineveld, D. J., Both, G. I. A., Fiksinski, A. M., Vorstman, J. A. S., Verhoeven-Duif, N. M., & Zinkstok, J. R. (2021). Psychiatric phenotypes associated with hyperprolinemia: A systematic review. *American Journal of Medical Genetics Part B: Neuropsychiatric Genetics*, *186*(5), 289–317.

Neumann-Staubitz, P., & Neumann, H. (2016). The use of unnatural amino acids to study and engineer protein function. *Current Opinion in Structural Biology*, *38*, 119–128.

Ng, P. C., & Henikoff, S. (2003). SIFT: Predicting amino acid changes that affect protein function. *Nucleic Acids Research*, *31*(13), 3812–3814.

Ng, P. C., & Henikoff, S. (2006). Predicting the effects of amino acid substitutions on protein function. *Annu. Rev. Genomics Hum. Genet.*, *7*, 61–80.

Öncel, P., Çetin, K., Topçu, A. A., Yavuz, H., & Denizli, A. (2017). Molecularly imprinted cryogel membranes for mitomycin C delivery. *Journal of Biomaterials Science, Polymer Edition*, *28*(6), 519–531.

Paksoy, H., Şahan, N., & Konuklu, Y. (2022). *Encapsulation of Phase Change Materials*.

Patriarca, E. J., Cermola, F., D'Aniello, C., Fico, A., Guardiola, O., De Cesare, D., & Minchiotti, G. (2021). The multifaceted roles of proline in cell behavior. *Frontiers in Cell and Developmental Biology*, *9*, 728576.

Ponrasu, T., Jamuna, S., Mathew, A., Madhukumar, K. N., Ganeshkumar, M., Iyappan, K., & Suguna, L. (2013). Efficacy of L-proline administration on the early responses during cutaneous wound healing in rats. *Amino Acids*, *45*, 179–189.

Ramanathan, S., Gopinath, S. C. B., Arshad, M. K. M., Poopalan, P., & Perumal, V. (2021). Nanoparticle synthetic methods: Strength and limitations. In *Nanoparticles in Analytical and Medical Devices* (pp. 31–43). Elsevier.

Rico-Yuste, A., & Carrasco, S. (2019). Molecularly imprinted polymer-based hybrid materials for the development of optical sensors. *Polymers*, *11*(7), 1173.

Sajid, M., & Płotka-Wasylka, J. (2020). Nanoparticles: Synthesis, characteristics, and applications in analytical and other sciences. *Microchemical Journal*, *154*, 104623.

Sandlers, Y. (2019). Amino acids profiling for the diagnosis of metabolic disorders. *Biochemical Testing-Clinical Correlation and Diagnosis*, 1–22.

Santos, C. S. C., Gabriel, B., Blanchy, M., Menes, O., García, D., Blanco, M., Arconada, N., & Neto, V. (2015). Industrial applications of nanoparticles–a prospective overview. *Materials Today: Proceedings*, *2*(1), 456–465.

Shahcheraghi, N., Golchin, H., Sadri, Z., Tabari, Y., Borhanifar, F., & Makani, S. (2022). Nano-biotechnology, an applicable approach for sustainable future. *3 Biotech*, *12*(3), 65.

Shoaib, A., Darraj, A., Khan, M. E., Azmi, L., Alalwan, A., Alamri, O., Tabish, M., & Khan, A. U. (2023). A Nanotechnology-Based Approach to Biosensor Application in Current Diabetes Management Practices. *Nanomaterials*, *13*(5), 867.

Sierra, A. F., Aragay, G., Peñuelas-Haro, G., & Ballester, P. (2021). Supramolecular fluorescence sensing of l-proline and l-pipecolic acid. *Organic Chemistry Frontiers*, *8*(11), 2402–2412.

Simonian, A. L., Rainina, E. I., Lozinsky, V. I., Badalian, I. E., Khachatrian, G. E., Tatikian, S. S., Makhlis, T. A., & Varfolomeyev, S. D. (1992). A biosensor for L-proline determination by use of immobilized microbial cells. *Applied Biochemistry and Biotechnology*, *36*, 199–210.

Sim, S., & Wong, N. K. (2021). Nanotechnology and its use in imaging and drug delivery. *Biomedical Reports*, *14*(5), 1–9.

Singabraya, D., Bultel, L., Siñeriz, F., Mothéré, M., Lesur, D., Kovensky, J., & Papy-Garcia, D. (2012). Molecular imprinting technology for specific recognition of heparan sulfate like disaccharides. *Talanta*, *99*, 833–839. https://doi.org/10.1016/j.talanta.2012.07.037

Song, J.-H., Min, S.-H., Kim, S.-G., Cho, Y., & Ahn, S.-H. (2022). Multi-functionalization strategies using nanomaterials: A review and case study in sensing applications. *International Journal of Precision Engineering and Manufacturing-Green Technology*, *9*(1), 323–347.

Srinivas, V., & Balasubramanian, D. (1995). Proline is a protein-compatible hydrotrope. *Langmuir*, *11*(7), 2830–2833.

Steinmann, B., Royce, P. M., & Superti-Furga, A. (2002). The Ehlers-Danlos syndrome. *Connective Tissue and Its Heritable Disorders: Molecular, Genetic, and Medical Aspects*, 431–523.

Su, S., & M Kang, P. (2020). Recent advances in nanocarrier-assisted therapeutics delivery systems. *Pharmaceutics*, *12*(9), 837.

Szabados, L., & Savouré, A. (2010a). Proline: a multifunctional amino acid. *Trends in Plant Science*, *15*(2), 89–97.

Szabados, L., & Savouré, A. (2010b). Proline: a multifunctional amino acid. *Trends in Plant Science*, *15*(2), 89–97.

Takahashi, T., Toda, E., B Singh, R., De Meester, F., Wilczynska, A., Wilson, D., & R Juneja, L. (2011). Essential and non-essential amino acids in relation to glutamate. *The Open Nutraceuticals Journal*, *4*(1).

Tan, C. J., & Tong, Y. W. (2007). Molecularly imprinted beads by surface imprinting. *Analytical and Bioanalytical Chemistry*, *389*, 369–376.

Taylor, W. R. (1986). The classification of amino acid conservation. *Journal of Theoretical Biology*, *119*(2), 205–218.

Thwala, L. N., Ndlovu, S. C., Mpofu, K. T., Lugongolo, M. Y., & Mthunzi-Kufa, P. (2023). Nanotechnology-Based Diagnostics for Diseases Prevalent in Developing Countries: Current Advances in Point-of-Care Tests. *Nanomaterials*, *13*(7), 1247.

Troll, W., & Lindsley, J. (1955). A photometric method for the determination of proline. *Journal of Biological Chemistry*, *215*(2), 655–660.

Van Hove, J. L. K., & Thomas, J. A. (2013). Disorders of glycine, serine, GABA, and proline metabolism. In *Physician's Guide to the Diagnosis, Treatment, and Follow-Up of Inherited Metabolic Diseases* (pp. 63–83). Springer.

Vasapollo, G., Sole, R. Del, Mergola, L., Lazzoi, M. R., Scardino, A., Scorrano, S., & Mele, G. (2011). Molecularly imprinted polymers: present and future prospective. *International Journal of Molecular Sciences*, *12*(9), 5908–5945.

Vettore, L. A., Westbrook, R. L., & Tennant, D. A. (2021). Proline metabolism and redox; maintaining a balance in health and disease. *Amino Acids*, *53*(12), 1779–1788.

Volkenstein, M. V. (1965). Coding of polar and non-polar amino-acids. *Nature*, *207*(4994), 294–295.

Wang, Q., Lin, X., Guo, D., Xu, J., Xuan, C., Chen, C., & Fu, Y. (2015). A novel chiral electrochemiluminescence sensor that can discriminate proline enantiomers. *RSC Advances*, *5*(114), 94338–94343.

Wang, R. Y., Wilcox, W. R., & Cederbaum, S. D. (2013). Amino acid metabolism. *Emery Rimoin's Essent. Med. Genet.*, *372*, 1–42.

Watkins, L. P., Chang, H., & Yang, H. (2006). Quantitative single-molecule conformational distributions: a case study with poly-(L-proline). *The Journal of Physical Chemistry A*, *110*(15), 5191–5203.

Wong, I. Y., Bhatia, S. N., & Toner, M. (2013). Nanotechnology: emerging tools for biology and medicine. *Genes & Development*, *27*(22), 2397–2408.

Wu, G. (2009). Amino acids: metabolism, functions, and nutrition. *Amino Acids*, *37*, 1–17.

Wu, G., Bazer, F. W., Burghardt, R. C., Johnson, G. A., Kim, S. W., Knabe, D. A., Li, P., Li, X., McKnight, J. R., & Satterfield, M. C. (2011). Proline and hydroxyproline metabolism: implications for animal and human nutrition. *Amino Acids*, *40*, 1053–1063.

Wulff, G. (1993). The role of binding-site interactions in the molecular imprinting of polymers. *Trends in Biotechnology*, *11*(3), 85–87.

Wulff, G. (1995). Molecular imprinting in cross-linked materials with the aid of molecular templates—a way towards artificial antibodies. *Angewandte Chemie International Edition in English*, *34*(17), 1812–1832.

Wulff, G., & Knorr, K. (2001). Stoichiometric noncovalent interaction in molecular imprinting. *Bioseparation*, *10*, 257–276.

Wu, Y., Zhai, Y., Zhang, Y., Zhang, H., Jing, H., & Chen, A. (2014). Chiral separation and determination of amino acids in real samples by LE-MEKC using Cu (II)-l-proline as chiral selector. *Journal of Chromatography B*, *965*, 254–259.

Wyse, A. T. S., & Netto, C. A. (2011). Behavioral and neurochemical effects of proline. *Metabolic Brain Disease*, *26*, 159–172.

Yahya, M. Z., & Abdullah, N. (2017). Preparation and Characterization of Hypercrosslinked Poly (HEMA-co-EGDMA-co-VBC). *Indian J. Sci. Technol*, *10*, 1–9.

Yan, H., & Row, K. H. (2006). Characteristic and synthetic approach of molecularly imprinted polymer. *International Journal of Molecular Sciences*, *7*(5), 155–178.

Yao, Y., & Han, W. (2022). Proline Metabolism in Neurological and Psychiatric Disorders. *Molecules and Cells*, *45*(11), 781.

Ye, L., Cormack, P. A. G., & Mosbach, K. (1999). Molecularly imprinted monodisperse microspheres for competitive radioassay. *Analytical Communications*, *36*(2), 35–38. https://doi.org/10.1039/a809014i

Yıldırım, M., & Baydemir Peşint, G. (2021). Molecularly imprinted spongy columns for Angiotensin(II) recognition from human serum. *Biotechnology Progress*, *37*(2). https://doi.org/10.1002/btpr.3112

Zenger, O., & Peşint, G. B. (2022). Preparation of molecularly imprinted bilayer cryogel columns for selective protein depletion. *Process Biochemistry*, *117*, 90–100.

Zhang, M., Wan, F., Wang, S., Ge, S., Yan, M., & Yu, J. (2012). Determination of l-proline based on anodic electrochemiluminescence of CdTe quantum dots. *Journal of Luminescence*, *132*(4), 938–943.

Zhang, Y., Pan, Z., Yuan, Y., Sun, Z., Ma, J., Huang, G., Xing, F., & Gao, J. (2013). Molecularly imprinted photonic crystals for the direct label-free distinguishing of L-proline and D-proline. *Physical Chemistry Chemical Physics*, *15*(40), 17250–17256.

Zharkova, M. S., Kopeykin, P. M., Afinogenov, G. E., Orlov, D. S., Artamonov, A. Y., Safiullina, K. E., Sukhareva, M. S., Tsvetkova, E. V, Milman, B. L., & Afinogenova, A. G. (2018). Effects of proline-rich peptides of the innate immune system on drug-resistant bacterial strains. *Meditsinskaya Immunologiya*, *20*(1), 107.

Zink, S., Moura, F. A., da Silva Autreto, P. A., Galvao, D. S., & Mizaikoff, B. (2018). Efficient prediction of suitable functional monomers for molecular imprinting via local density of states calculations. *Physical Chemistry Chemical Physics*, *20*(19), 13153–13158.